Journal of Fluids and Structures 17 (2003) 185–224

JOURNAL OF FLUIDS AND STRUCTURES

www.elsevier.nl/locate/jnlabr/yjfls

# Large strain formulations of extensible flexible marine pipes transporting fluid

S. Chucheepsakul[a,*], T. Monprapussorn[a], T. Huang[b]

[a] Department of Civil Engineering, King Mongkut's University of Technology Thonburi, Bangmod, Toongkru, Bangkok 10140, Thailand
[b] Department of Civil and Environmental Engineering, University of Texas at Arlington, Arlington, TX 76019-0167, USA

Received 15 August 2000; accepted 8 August 2002

**Abstract**

This paper develops mathematical formulations for large strain analysis of extensible flexible marine pipes transporting fluid in two different coordinates: Cartesian and natural coordinates. Both the virtual work method and the vectorial method are applied to generate the large strain formulations, in which deformation descriptions based upon the total Lagrangian, the updated Lagrangian, and the Eulerian mechanics are taken into consideration. The new ideas used in the model formulations deal with applications of the extensible elastica theory and the apparent tension concept to handle combined action of the effect of axial deformation with large strain and behaviour of flow of transported fluid inside the pipe including the effect of Poisson's ratio. The present models cover nonlinear statics and nonlinear dynamics, and provide flexibility in the choice of the independent variables used to define the elastic curves.


## 1. Introduction

In the past five decades, flexible pipes have been employed extensively in numerous offshore engineering applications. The most vital function of them is to transport fluids drilled from underneath ocean floor such as oil, gas, hydrocarbon, and other crude resources, up to the production platform or drilling ship. In the deep-ocean mining industry, flexible pipes play the role of the main module of the production system as shown in Fig. 1(a). In moderate sea-depth applications, they are often used as the secondary part, linked to rigid risers as shown in Fig. 1b and c.

In the literature, there are many papers related to flexible pipe analysis as reviewed by Chakrabarti and Frampton (1982), Ertas and Kozik (1987), Jain (1994) and Patel and Seyed (1995). It is remarkable that most of them omit the effect of axial deformation of the pipe, and the influence of internal flow. Furthermore, all of them overlook the Poisson's ratio effect. As will be reviewed and discussed later, the individual effect of axial deformation, internal flow, and Poisson's ratio can be significant for behaviour of low flexibility pipes. It is therefore conceivable that combined actions of all the effects become more important for behaviour of highly flexible pipes. In such cases, those effects should be carefully examined, and large strain analysis is essential.

However, hitherto a mathematical treatment for the large strain analysis that takes into consideration the combined actions of those effects has not been elucidated. Hence it is the objective of this paper: first to introduce and explain the mathematical principles for large strain analysis of extensible flexible marine pipes conveying fluid from viewpoints of the total Lagrangian, the updated Lagrangian, and the Eulerian mechanics; second to show how to formulate large strain models of marine pipes in Cartesian and natural coordinates by relying upon the extensible elastica theory and

*Corresponding author. Tel.: +662-470-9134-36; fax: +662-427-9063.
*E-mail address:* somchai.chu@kmutt.ac.th (S. Chucheepsakul).

0889-9746/03/$ - see front matter 
PII: S0889-9746(02)00116-0

**Nomenclature**

$\bar{A}_e, A_{eo}, A_e$ sectional areas of the external fluid column at the three states
$\bar{A}_i, A_{io}, A_i$ sectional areas of the internal fluid column at the three states
$\bar{A}_P, A_{Po}, A_p$ sectional areas of a pipe at the three states
$\mathbf{a}_F, \mathbf{a}_{FP}$ acceleration vectors of transported fluid relative to a fixed frame and a pipe
$a_{Fn}, a_{Ft}, a_{Fx}, a_{Fy}$ accelerations of transported fluid relative to a fixed frame in normal, tangential, horizontal, and vertical directions, respectively
$\mathbf{a}_P$ acceleration vector of a pipe relative to a fixed frame
$a_{Pn}, a_{Pt}, a_{Px}, a_{Py}$ accelerations of a pipe relative to a fixed frame in normal, tangential, horizontal, and vertical directions, respectively
$\bar{B}, B_o, B$ bending rigidities at the three states
$C_{Dn}, C_{Dt}, C_a, C_M$ coefficients of normal drag, tangential drag, added mass, and inertia
$\bar{D}_e, D_{eo}, D_e$ diameters of the external fluid column at the three states
$\bar{D}_P, D_{Po}, D_P$ diameters of a pipe at the three states
$E$ elastic modulus
$\bar{\mathbf{f}}, \mathbf{f}_o, \mathbf{f}$ external load vectors at the three states
$\bar{\mathbf{f}}_H, \mathbf{f}_{Ho}, \mathbf{f}_H$ hydrodynamic force vectors at the three states
$F_{Hn}, F_{Ht}, F_{Hx}, F_{Hy}$ hydrodynamic forces in normal, tangential, horizontal, and vertical directions, respectively
$f_{Hn}, f_{Ht}, f_{Hx}, f_{Hy}$ hydrodynamic forces per unit length in normal, tangential, horizontal, and vertical directions, respectively
$F_{IPn}, F_{Iin}, F_{In}$ normal inertial forces of a pipe, transported fluid, and overall system
$F_{IPt}, F_{Iit}, F_{It}$ tangential inertial forces of a pipe, transported fluid, and overall system
$f_{rn}$ normal reaction between pipe wall and transported fluid per unit length
$f_n, f_t, f_x, f_y$ external load components in Eqs. (123c) and (129g)
$g$ gravitational acceleration
$\bar{H}, H_o, H$ horizontal internal forces at the three states
$\hat{\mathbf{i}}, \hat{\mathbf{j}}$ horizontal and vertical unit vectors in Cartesian system
$\bar{I}_P, I_{Po}, I_P$ moments of inertia of a pipe at the three states
$\bar{M}, M_o, M$ bending moments at the three states
$\bar{N}, N_o, N$ axial forces at the three states
$\bar{m}_e, m_{eo}, m_e$ masses of the external fluid column per unit length at the three states
$\bar{m}_i, m_{io}, m_i$ masses of the internal fluid column per unit length at the three states
$\bar{m}_P, m_{Po}, m_P$ masses of a pipe per unit length at the three states
$\bar{\mathbf{n}}, \hat{\mathbf{n}}_o, \hat{\mathbf{n}}$ normal unit vectors in natural system at the three states
$p_e, p_i$ pressures of external and internal fluids
$\bar{Q}, Q_o, Q$ shear forces at the three states
$\bar{r}, r_o, r$ radii of curvatures at the three states
$\mathbf{r}_F, \mathbf{r}_{FP}$ position vectors of transported fluid relative to a fixed frame and a pipe
$\mathbf{r}_P$ position vector of a pipe relative to a fixed frame
$\bar{s}, s_o, s$ arc-length coordinates at the three states
$\bar{T}, T_o, T$ true wall tensions at the three states
$\bar{T}_a, T_{ao}, T_a$ apparent tensions at the three states
$\bar{T}_e, T_{eo}, T_e$ effective tensions at the three states
$T_{tri}$ apparent tension due to triaxial stress
$t$ time (time derivative denoted by overdot such as $\partial x/\partial t = \dot{x}$)
$\bar{\mathbf{t}}, \hat{\mathbf{t}}_o, \hat{\mathbf{t}}$ tangential unit vectors in natural system at the three states
$\mathbf{u}_o, \mathbf{u}$ displacement vectors from state 1 to 2 and state 2 to 3
$u_o, u$ horizontal displacements from state 1 to 2 and state 2 to 3
$u_{no}, u_n$ normal displacements from state 1 to 2 and state 2 to 3
$\bar{V}, V_o, V$ vertical internal forces at the three states
$V_{ct}, V_c$ current velocities at mean sea level and at any sea depth
$\mathbf{V}_F, \mathbf{V}_{FP}$ velocity vectors of transported fluid relative to a fixed frame and a pipe
$V_{Hn}, V_{Ht}$ external hydrodynamic velocities in normal and tangential directions

$V_{Hx}, V_{Hy}$ external hydrodynamic velocities in horizontal and vertical directions
$\bar{V}_i, V_{io}, V_i$ internal flow velocities at the three states
$\mathbf{V}_P$ velocity vector of a pipe relative to a fixed frame
$V_{Px}, V_{Py}, V_{P\theta}$ horizontal, vertical, and rotational velocities of a pipe
$V_w$ wave velocity
$v_o, v$ vertical displacements from state 1 to 2 and state 2 to 3
$v_{no}, v_n$ tangential displacements from state 1 to 2 and state 2 to 3
$W_P, W_e, W_i$ weights of a pipe, the external fluid column, and the internal fluid column
$\bar{w}_a, w_{ao}, w_a$ apparent weights per unit length at the three states
$\mathbf{x}_o, \mathbf{x}$ Cartesian vectors of displacements from state 1 to 2 and state 2 to 3
$\bar{x}, x_o, x$ horizontal Cartesian coordinates at the three states
$\bar{x}_t$ static offset
$\bar{y}, y_o, y$ vertical Cartesian coordinates at the three states
$\bar{y}_b, \bar{y}_t$ vertical distances from bottom support to seabed and to sea surface

*Greek symbols*
$\alpha$ independent variable (its derivative $\partial/\partial\alpha$ denoted by ($'$))
$\gamma_A, \gamma_G$ Almansi's and Green's strains
$\gamma, \gamma_o, \gamma_d$ total, static, and dynamic updated Green strains
$\gamma_n, \gamma_t$ relative velocities of external fluid in normal and tangential directions
$\bar{\varepsilon}, \varepsilon_o, \varepsilon$ axial strains at the three states
$\varepsilon$, $\varepsilon_o$, $\varepsilon_d$ total, static, and dynamic axial strains ($\varepsilon_d = \varepsilon - \varepsilon_o$)
$\varepsilon_{tri}$ axial strain due to the tension $T_{tri}$
$\bar{\varepsilon}_v, \varepsilon_{vo}, \varepsilon_v$ volumetric strains of a pipe at the three states
$\varepsilon_\varsigma$ axial strain at a fibre radius coordinate $\varsigma$
$\varsigma$ a fibre radius coordinate
$\bar{\theta}, \theta_o, \theta$ rotational angles at the three states
$\bar{\kappa}, \kappa_o, \kappa$ curvatures at the three states
$v$ Poisson's ratio
$\pi_{an}, \pi_{at}, \pi_{ax}, \pi_{ay}$ total virtual works of apparent system in normal, tangential, horizontal, and vertical directions, respectively
$\rho_P, \rho_e, \rho_i$ densities of a pipe, external fluid, and internal fluid
$\sigma_P$ end effect stress
$\sigma_t, \sigma_\theta, \sigma_r$ triaxial stress in Fig. 4(f)
$\tau$ shear stress in pipe wall
$\tau_w$ wall shear friction between pipe wall and transported fluid
$\bar{\forall}_{cv}, \forall_{cv}, \forall_{cv}$ control volumes of a pipe at the three states
$\bar{\forall}_e, \forall_{eo}, \forall_e$ volumes of the external fluid column at the three states
$\bar{\forall}_i, \forall_{io}, \forall_i$ volumes of the internal fluid column at the three states
$\bar{\forall}_P, \forall_{Po}, \forall_P$ volumes of a pipe at the three states

*Subscripts*
$P$ pipe
$e$ external fluid
$i$ internal fluid
$o$ static quantity
$d$ dynamic quantity
$n$ natural coordinates.

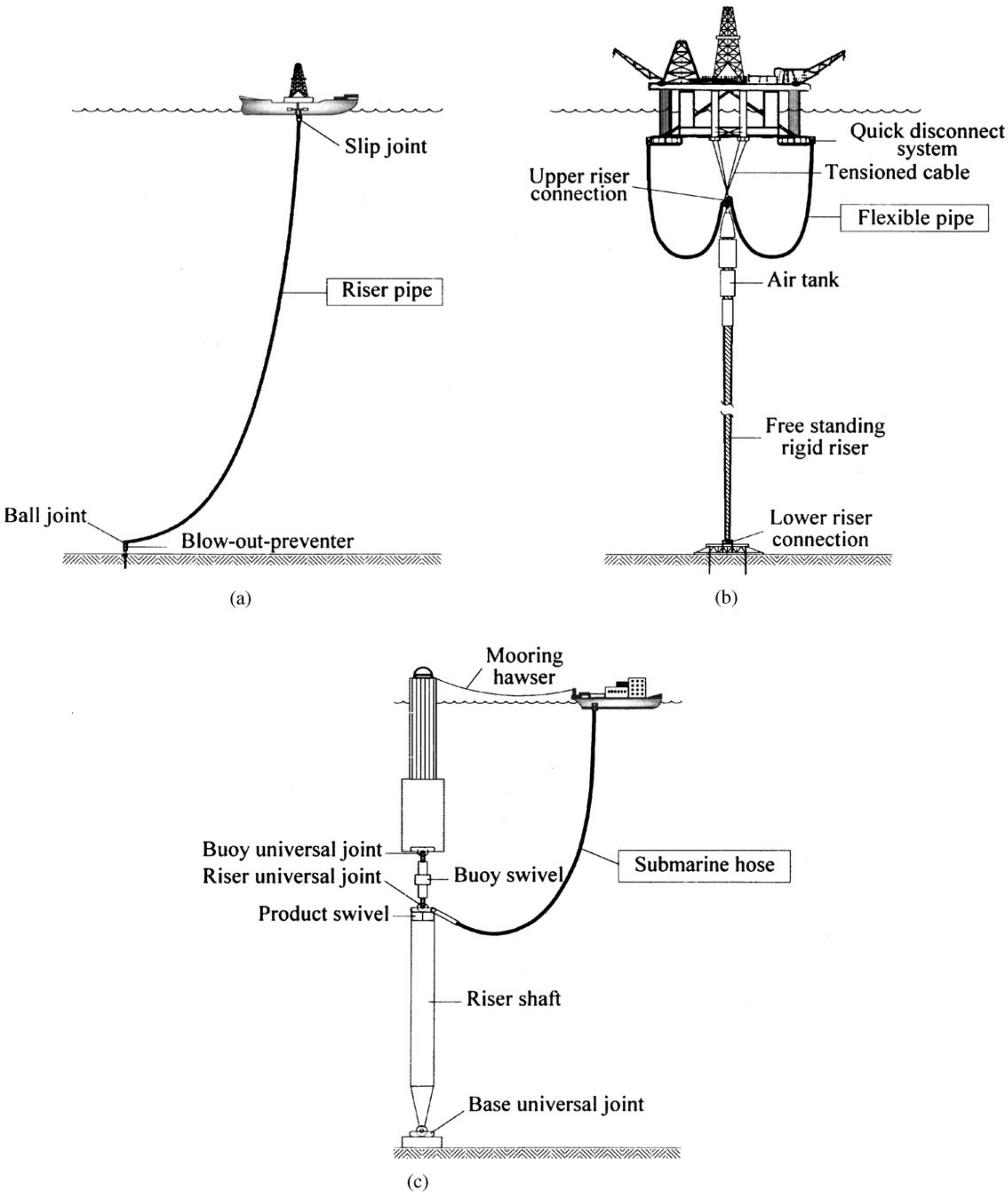


Fig. 1. Flexible marine pipes: (a) marine riser; (b) flexible pipe; and (c) hoseline.

the apparent tension concept; and finally to illustrate versatile and sophisticated models suitable for two-dimensional large strain analysis of extensible flexible marine pipes conveying fluid.

### 1.1. Significance of effect of axial deformation

From a literature review, the effect of axial deformation on behaviour of marine cables was investigated by Huang (1992), Chucheepsakul et al. (1995) and Chucheepsakul and Huang (1997). The effect on behaviour of suspended cables was studied by Huddleston (1981), Shih and Tadjbakhsh (1984), Burgess and Triantafyllou (1988), Lin and Perkins

(1995), Triantafyllou and Yue (1994) and Tjavaras et al. (1996, 1998). The effect was included in analysis of low flexibility marine risers by Chung and Whitney (1983), Chung et al. (1994), Chung and Cheng (1996) and Bernitsas and Kokarakis (1988); Bernitsas et al. (1985).

It was reported that the effect of axial deformation on static behaviour of those structures is to increase static displacements of low-tensioned cables, due to extensibility dominating; but to reduce the static displacement of high-tensioned cables, due to pre-stressing dominating (Chucheepsakul et al., 1995; Chucheepsakul and Huang, 1997). Although Bernitsas and Kokarakis (1988); Bernitsas et al. (1985) found that the effect on static behaviour of low flexibility pipes was rather small, they did not provide evidence of the same result with the highly flexible pipes.

In relation to the dynamic behaviour of these structures, the effect of axial deformation is to increase dynamic stresses (Chung and Whitney, 1983; Chung et al. (1994); Chung and Cheng, 1996), to reduce natural frequencies (Chucheepsakul and Huang, 1997), and to provoke elastic mode transition of cable vibrations (Burgess and Triantafyllou, 1988; Lin and Perkins, 1995). If the stress–strain relation is hysteretic, the effect can amplify damping of dynamic strain in the axial direction (Triantafyllou and Yue, 1994). Several papers by Chung and Whitney (1983), Chung et al. (1994), Chung and Cheng (1996) comment that the effect of axial deformation is crucial to dynamics of low flexibility pipes and should be considered in the design of the pipe.

The interesting point in all the previous research is that the effect of axial deformation has been investigated by using small-strain analysis that adopts quadratic expressions for strain definitions. This approach, however, is proper if, and only if, the axial strain is small compared to unity (Fung, 1994). For highly flexible pipes, such an assumption is no longer necessarily valid; thus, this paper proposes large strain modelling by employing the square-root expressions for large strain definitions, as will be shown later.

### *1.2. Significance of influence of internal flow*

Although transporting fluid is the main function, marine riser pipe analysis from the middle of the 1950s to the end of the 1970s paid little attention to the influence of transported fluid. In the same period, research concerning mechanics of pipes conveying fluid grew rapidly. Research work related to vibrations of straight and curved pipes can be found in the papers by Housner (1952), Gregory and Païdoussis (1966), Païdoussis (1970) and Doll and Mote (1976). It was reported that the internal flow reduced stability of the pipe and acted on the pipe like an end follower force (Thompson and Lunn, 1981). As a result, it could engender divergence instability or buckling of simply supported pipes (Holmes, 1978), and could induce flutter instability or snaking behaviour of cantilever pipes (Gregory and Païdoussis, 1966).

The lack of connection between research work on marine pipes and pipes conveying fluid has led to a misconception amongst some authors. When the effect of internal flow on marine pipes was handled in the early 1980s, it was considered that internal flow induced only friction forces to act on the pipe wall. However, researchers concerned with pipes conveying fluid, such as Gregory and Païdoussis (1966), Païdoussis (1970), and Thompson and Lunn (1981), had been well aware that the internal friction forces did not act directly on the pipe, but they affected the internal pressure transmitted to the pipe wall, which yielded tensioning and pressure drop (Païdoussis, 1998). In addition, internal flow generates not only the pressure effects, but also the other fictitious forces such as Coriolis and centrifugal forces.

By the end of the 1980s, the effect of internal flow on behaviour of marine pipes began to draw specific interest from a number of researchers, and the misconception was remedied. It was reported that internal flow reduced structural stiffness, provided negative damping (Irani et al., 1987), and induced additional large displacements of the pipes (Chucheepsakul and Huang, 1994); reduction of natural frequencies of the pipes is slight at a low speed of internal flow, but significant at a high speed of internal flow (Moe and Chucheepsakul, 1988; Wu and Lou, 1991); internal slug flow can induce significant cyclic fatigue loading in deep water (Patel and Seyed, 1989); and simply supported marine riser pipes transporting fluid lost stability by divergence (Chucheepsakul et al., 1999).

However, mathematical models used in most of those works do not consider the effects of geometric nonlinearity, extensibility, and the Poisson's ratio effect on the pipes, despite the fact that flexible marine pipes are inclined, initially curved, significantly deflected and deformed. This shortcoming motivates the aim of this work to exhibit how to take into account these effects in large strain formulations of flexible marine pipes conveying fluid. Revealing the interaction between the transported fluid and the pipe subjected to these effects provides new understanding of the behaviour of such systems.

### *1.3. Significance of Poisson's ratio effect and fluid pressures*

It will be shown later that the Poisson's ratio effect and lateral actions of fluid pressures disturb the behaviour of flexible marine pipes in three ways: first, altering structural stiffness; second, modifying internal flow characteristics; and third, varying the apparent tension in the pipe.

A review of the literature shows that while the first two effects have not been examined in marine pipe analysis, the first effect has been included in marine cable analysis by Goodman and Breslin (1976). Even if the third effect on the flexible marine pipes has been treated through the effective tension concept proposed by Sparks (1984), the Poisson's ratio effect is not fully taken into account.

As will be shown later, using the effective tension concept creates an error in evaluating the apparent tension arising in the cross-section of the pipe, whenever the Poisson's ratio is not equal to 0.5. The greater the difference of Poisson's ratio from 0.5, the higher the error grows, especially under a condition of severe fluid pressures. In order to avoid such an error, this paper establishes the apparent tension concept instead of the effective tension concept. The detailed treatments of the first two effects on mathematical models for large strain analysis of flexible marine pipes are also included.

### 1.4. Assumptions

The following assumptions are stipulated in the present mathematical modelling:

(a) The pipe materials are linearly elastic. Therefore, the Kelvin–Voigt internal dissipation or the dissipative recovery is not relevant.
(b) At the undeformed state, the pipes are initially straight, and have no residual stresses.
(c) The pipes are sufficiently thick-walled to suppose that, ideally, their cross-sections remain circular after change of cross-sectional size due to the Poisson's ratio effect, so that the elastic rod theories are usable, and Brazier's effect or flattening of bent tubes is negligible.
(d) Longitudinal strain is large, but shear strain is insignificant for elastic rods with high slenderness ratio.
(e) Plane sections of the pipes remain plane at all states.
(f) The internal and external fluids are inviscid, incompressible, and irrotational. Their densities are uniform along arc lengths of the pipes.
(g) The internal flow is the one-dimensional plug laminar flow.
(h) The general form of Morison's equation is adopted for evaluating external hydrodynamic forces of external fluid. The distributed couple induced by a flow asymmetry due to vortex shedding is neglected.
(i) The effect of rotary inertia is negligible.

## 2. Fundamentals of large strain modelling of flexible marine pipes conveying fluid

Large displacement behaviour of an extensible flexible marine pipe is depicted in Fig. 2. Firstly, the pipe is at rest and unstretched at state 1: *the undeformed state*. Subsequently, as the pipe is subjected to time-independent loads due to gravitation, steady current flow, and steady internal flow, the pipe experiences large displacement and forms the initial condition of the pipe at state 2: *the equilibrium state*. Finally, under dynamic actions of disturbances such as waves, unsteady current, and unsteady internal flow, the pipe sustains vibration about the equilibrium configuration at state 3: *the displaced state*.

Corresponding to the three states, mathematical treatments of the following subjects are considered to be requisite for large strain analysis of extensible marine pipes transporting fluid: (1) physical descriptions, (2) large strain measurements, (3) the extensible elastica theory, (4) the apparent tension concept, and (5) dynamic interactions between fluids and pipes. Details of these subjects are given as follows.

### 2.1. Physical descriptions

In order to define positions, motions, and deformations of an extensible flexible pipe and transported fluid, the descriptions for geometry, kinematics, and deformation are necessary for large strain modelling.

(a) *Geometric description*. Fig. 2 uses the Cartesian coordinates $(\hat{\mathbf{i}}, \hat{\mathbf{j}})$ and the intrinsic coordinates of arc length and rotation $(\hat{\mathbf{s}}, \hat{\theta})$ as the global geometric descriptors, and employs the natural coordinates $(\hat{\mathbf{n}}, \hat{\mathbf{t}})$ as the local geometric descriptor. From the two global systems, there exist a number of choices of the independent variable. For versatility of mathematical models, the symbol $\alpha \in \{\bar{x}, x_o, x, \bar{y}, y_o, y, \bar{s}, s_o, s, \bar{\theta}, \theta_o, \theta\}$ is introduced to represent any independent variable, and the superscript $(')$ denotes $\partial()/\partial\alpha$.
(b) *Kinematic and deformation descriptions*. As shown in Fig. 3, there may be three ways to describe motions and deformations of a pipe and transported fluid. These involve the descriptions by total Lagrangian, updated Lagrangian, and Eulerian coordinates as follows.

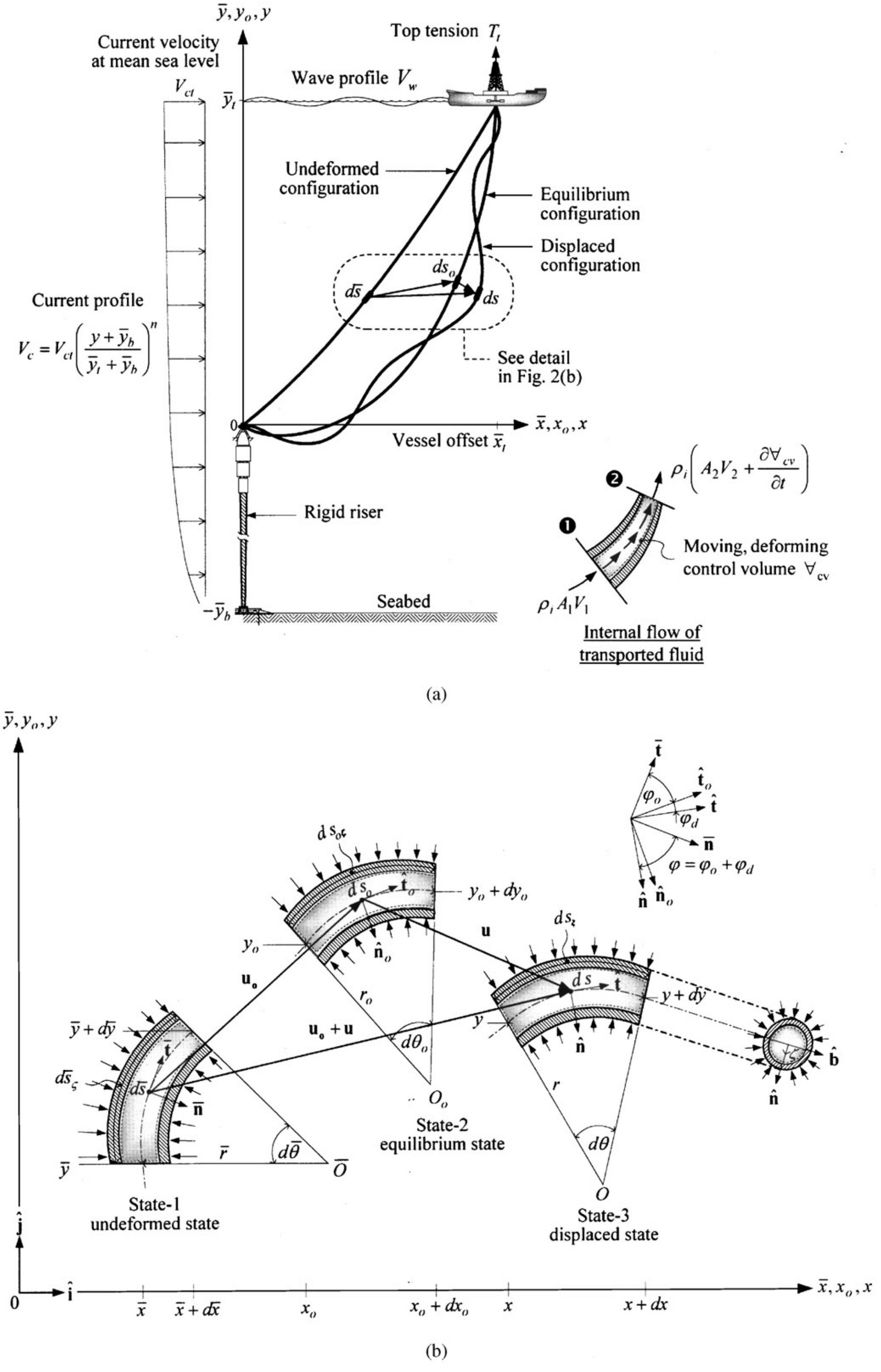


Fig. 2. Schematics of large displacements and large deformations.

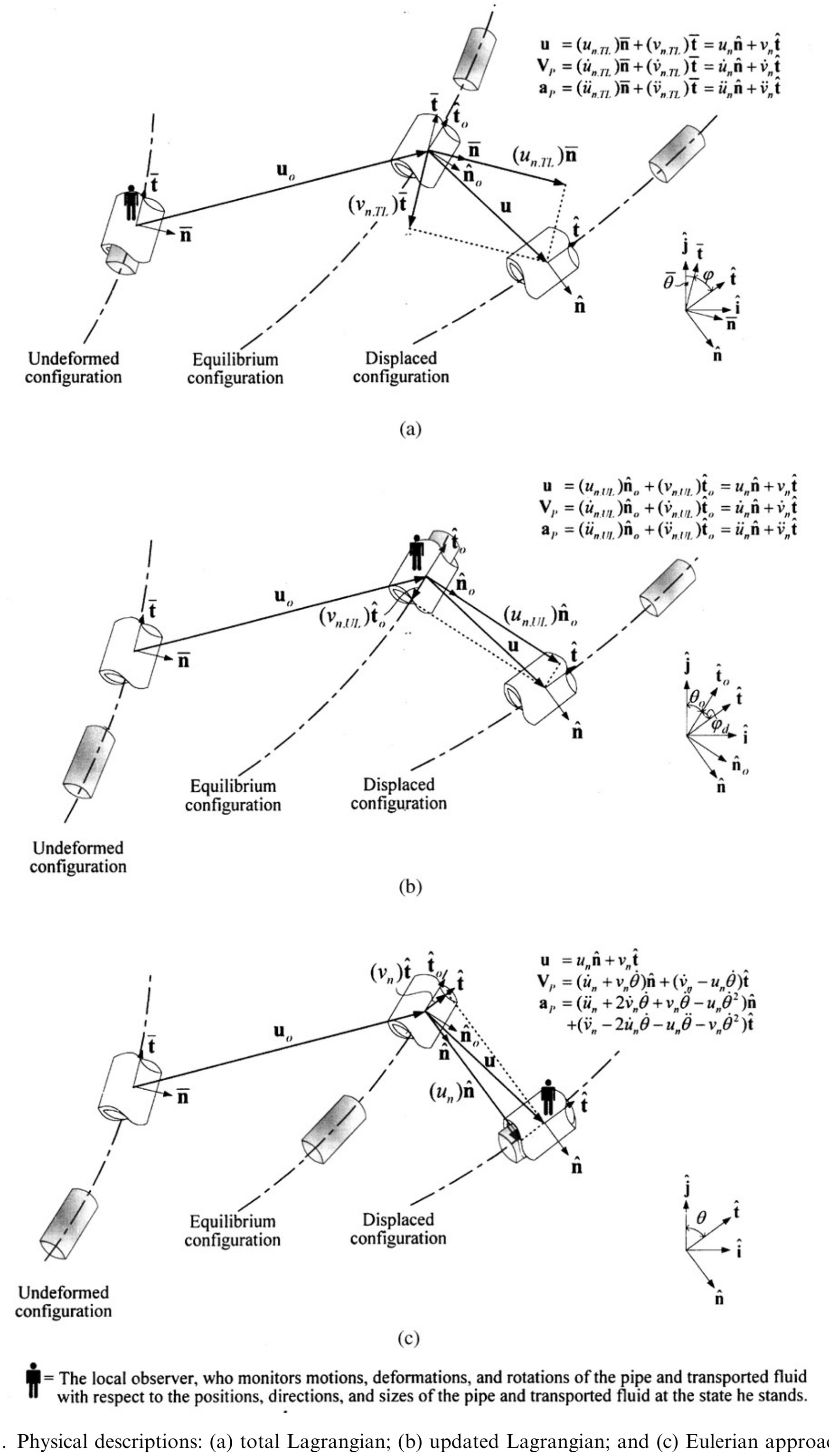


Fig. 3. Physical descriptions: (a) total Lagrangian; (b) updated Lagrangian; and (c) Eulerian approaches.

**Definition 1.** The coordinate that follows motion and deformation of a deformable body with respect to position, direction, and size of the body at the original state (or the undeformed state herein) is said to be *the total Lagrangian descriptor* (*TL*) as shown in Fig. 3(a).

**Definition 2.** The coordinate that follows motion and deformation of a deformable body with respect to position, direction, and size of the body at the intermediate state (or the equilibrium state herein) is said to be *the updated Lagrangian descriptor* (*UL*) as shown in Fig. 3(b).

**Definition 3.** The coordinate that follows motion and deformation of a deformable body with respect to position, direction, and size of the body at the final state (or the displaced state herein) is said to be *the Eulerian descriptor* (*EL*) as shown in Fig. 3(c).

### 2.2. Large strain measurements

Corresponding to the three deformation descriptors defined in the previous section, definitions of the total axial strain $\varepsilon$, the static strain $\varepsilon_o$, and the dynamic strain $\varepsilon_d$ can be provided in the following three forms.

(i) For deformation descriptor TL:

$$\varepsilon = \frac{s'}{\bar{s}'} - 1, \tag{1a}$$

$$\varepsilon_o = \frac{s'_o}{\bar{s}'} - 1, \tag{1b}$$

$$\varepsilon_d = \frac{s' - s'_o}{\bar{s}'}. \tag{1c}$$

(ii) For deformation descriptor UL:

$$\varepsilon = \frac{s' - \bar{s}'}{s'_o}, \tag{2a}$$

$$\varepsilon_o = 1 - \frac{\bar{s}'}{s'_o}, \tag{2b}$$

$$\varepsilon_d = \frac{s'}{s'_o} - 1. \tag{2c}$$

(iii) For deformation descriptor EL:

$$\varepsilon = 1 - \frac{\bar{s}'}{s'}, \tag{3a}$$

$$\varepsilon_o = \frac{s'_o - \bar{s}'}{s'}, \tag{3b}$$

$$\varepsilon_d = 1 - \frac{s'_o}{s'}. \tag{3c}$$

Note that $\varepsilon = \varepsilon_o + \varepsilon_d$, and the differential arc lengths at the undeformed, the equilibrium, and the displaced states $\bar{s}'$, $s'_o$, and $s'$ may be expressed as

$$\bar{s}' = \sqrt{\bar{x}'^2 + \bar{y}'^2}, \tag{4a}$$

$$s'_o = \sqrt{(\bar{x}' + u'_o)^2 + (\bar{y}' + v'_o)^2}, \tag{4b}$$

in Cartesian coordinates:

$$s' = \sqrt{(\bar{x}' + u'_o + u')^2 + (\bar{y}' + v'_o + v')^2}, \tag{4c}$$

in natural coordinates:

$$s' = \sqrt{(u'_n + v_n\theta'_o)^2 + (s'_o + v'_n - u_n\theta'_o)^2}. \tag{4d}$$

The large strain expressions given by Eqs. (1)–(3) can be exhibited in *classical square-root forms* of axial strains as follows.

**Definition 4.** The large axial strain for flexible pipe analysis is defined by

$$\varepsilon = \begin{cases} \dfrac{s'}{\bar{s}'} - 1 = \varepsilon_o + \left(\dfrac{s'}{s'_o} - 1\right)(1+\varepsilon_o) = \sqrt{1+2\gamma_G} - 1 & \text{for TL,} \\ \dfrac{s' - \bar{s}'}{s'_o} = \varepsilon_o + \left(\dfrac{s'}{s'_o} - 1\right) = \sqrt{1+2\gamma_d} - \sqrt{1-2\gamma_o} & \text{for UL,} \\ 1 - \dfrac{\bar{s}'}{s'} = \varepsilon_o + \left(1 - \dfrac{s'_o}{s'}\right) = 1 - \sqrt{1-2\gamma_A} & \text{for EL.} \end{cases} \tag{5a–c}$$

In other words, the large axial strains are measured by means of 'engineering strains' or 'relative elongations'. The square-root expressions in Eqs. (5) demonstrate that the large axial strains are functions of the lower-order axial strains such as the static updated Green strain $\gamma_o$, the dynamic updated Green strain $\gamma_d$, the total updated Green strain $\gamma$, the Green strain $\gamma_G$, and the Almansi strain $\gamma_A$. By substituting Eqs. (4) into Eqs. (5), and undertaking some manipulation, the expressions of these lower-order axial strains can be obtained as

$$\gamma_o = \frac{1}{s'^2_o}\left[\bar{x}'u'_o + \bar{y}'v'_o + \frac{u'^2_o}{2} + \frac{v'^2_o}{2}\right], \tag{6a}$$

in Cartesian coordinates:

$$\gamma_d = \frac{1}{s'^2_o}\left(x'_o u' + y'_o v' + \frac{u'^2}{2} + \frac{v'^2}{2}\right), \tag{6b}$$

in natural coordinates:

$$\gamma_d = \frac{1}{s'^2_o}\left[s'_o(v'_n - u_n\theta'_o) + \frac{(u'_n + v_n\theta'_o)^2}{2} + \frac{(v'_n - u_n\theta'_o)^2}{2}\right], \tag{6c}$$

$$\gamma = \gamma_o + \gamma_d, \quad \gamma_G = \gamma(s'_o/\bar{s}')^2, \quad \gamma_A = \gamma(s'_o/s')^2. \tag{6d–f}$$

For lower-order large strain analysis, the dynamic axial strains in Eqs. (5) may be approximated by the two-term binomial series such that

$$\frac{s'}{s'_o} = \sqrt{1+2\gamma_d} \approx 1 + \gamma_d, \quad \frac{s'_o}{s'} = \frac{1}{\sqrt{1+2\gamma_d}} \approx 1 - \gamma_d. \tag{7a–b}$$

Inserting Eqs. (7) into Eqs. (5), *the quadratic forms* of axial strains are derived as Definition 5.

**Definition 5.** The nonlinear second-order axial strain for flexible pipe analysis is defined by

$$\varepsilon \approx \begin{cases} \varepsilon_o + \gamma_d(1+\varepsilon_o) & \textit{for TL,} \\ \varepsilon_o + \gamma_d & \textit{for UL and EL,} \end{cases} \tag{8a, b}$$

to which quadratic expressions of $\gamma_d$ as shown in Eqs. (6b) and (6c) are applied.

For linear approximation, the second-order terms of $\gamma_d$ are negligible as higher-order terms, so that Eq. (6b) is linearized to

in Cartesian coordinates:

$$\gamma_d \simeq \frac{1}{s'_o 2}(x'_o u' + y'_o v'), \tag{9a}$$

in natural coordinates:

$$\gamma_d \simeq \frac{1}{s'_o}(v'_n - u_n\theta'_o). \tag{9b}$$

By utilizing Eq. (9), *the linear forms* of axial strains are derived as Definition 6.

**Definition 6.** The linear axial strain for flexible pipe analysis is defined by Eqs. (8), to which linear approximation of $\gamma_d$ by Eqs. (9) is applied.

The large strain definition (Definition 4) is considered necessary for nonlinear dynamic analysis of flexible pipes, in which large amplitude vibrations and large strain behaviour are concerned. The nonlinear second-order strain definition (Definition 5) is desired for nonlinear dynamic analysis of flexible pipes, in which large amplitude vibrations with large static and small dynamic strains are interested. The linear strain definition (Definition 6) is sufficient for dynamic stability analysis and linear dynamic problems of flexible pipes, to which large static and infinitesimal dynamic strains are relevant.

Variations of the axial strain among the three states bring about variations of differential arc length of the pipe, cross-sectional properties of the pipe, and internal flow velocity of transported fluid as follows.

(a) *Variations of differential arc length of the pipe*. By solving Eqs. (1a) and (1b) for $\bar{s}'$, solving Eqs. (2b) and (2c) for $s_o'$, and solving Eqs. (3a) and (3c) for $s'$, one obtains

$$\bar{s}' = \frac{s_o'}{1+\varepsilon_o} = \frac{s'}{1+\varepsilon} \quad \text{for TL,} \tag{10a}$$

$$\frac{\bar{s}'}{1-\varepsilon_o} = s_o' = \frac{s'}{1+\varepsilon_d} \quad \text{for UL,} \tag{10b}$$

$$\frac{\bar{s}'}{1-\varepsilon} = \frac{s_o'}{1-\varepsilon_d} = s' \quad \text{for EL.} \tag{10c}$$

(b) *Variations of cross-sectional properties of the pipe*. The volumetric strain of the pipe is expressed as

$$\varepsilon_v = \begin{cases} \dfrac{\mathrm{d}\forall_P - \mathrm{d}\bar{\forall}_P}{\mathrm{d}\bar{\forall}_P} = \dfrac{A_P s'}{\bar{A}_P \bar{s}'} - 1 = \dfrac{A_P}{\bar{A}_P}(1+\varepsilon) - 1 & \text{for TL,} \\ \dfrac{\mathrm{d}\forall_P - \mathrm{d}\bar{\forall}_P}{\mathrm{d}\forall_{Po}} = \dfrac{A_P s' - \bar{A}_P \bar{s}'}{A_{Po} s_o'} = \dfrac{A_P}{A_{Po}}(1+\varepsilon_d) - \dfrac{\bar{A}_P}{A_{Po}}(1-\varepsilon_o) & \text{for UL,} \\ \dfrac{\mathrm{d}\forall_P - \mathrm{d}\bar{\forall}_P}{\mathrm{d}\forall_P} = 1 - \dfrac{\bar{A}_P \bar{s}'}{A_P s'} = 1 - \dfrac{\bar{A}_P}{A_P}(1-\varepsilon) & \text{for EL.} \end{cases} \tag{11a–c}$$

Based on the control volume approach (Goodman and Breslin, 1976), the pipe volume is conserved, and thus the volumetric strain of the pipe $\varepsilon_v = \varepsilon_{vo} = 0$. Once these conditions are applied to Eqs. (11), the cross-sectional areas of the pipe at the three states can be related together as

$$\bar{A}_P = A_{Po}(1+\varepsilon_o) = A_P(1+\varepsilon) \quad \text{for TL,} \tag{12a}$$

$$\bar{A}_P = \frac{A_{Po}}{1-\varepsilon_o} = \frac{(1+\varepsilon_d)A_P}{(1-\varepsilon_o)} \quad \text{for UL,} \tag{12b}$$

$$\bar{A}_P = \frac{A_{Po}}{1-\varepsilon_o} = \frac{A_P}{1-\varepsilon} \quad \text{for EL.} \tag{12c}$$

Corresponding to Eqs. (12), variations of diameter and moment of inertia of the circular pipe among the three states are determined as

$$\bar{D}_P = D_{Po}\sqrt{1+\varepsilon_o} = D_P\sqrt{1+\varepsilon} \quad \text{for TL,} \tag{13a}$$

$$\bar{D}_P = \frac{D_{Po}}{\sqrt{1-\varepsilon_o}} = D_P\sqrt{\frac{1+\varepsilon_d}{1-\varepsilon_o}} \quad \text{for UL,} \tag{13b}$$

$$\bar{D}_P = \frac{D_{Po}}{\sqrt{1-\varepsilon_o}} = \frac{D_P}{\sqrt{1-\varepsilon}} \quad \text{for EL,} \tag{13c}$$

$$\bar{I}_P = I_{Po}(1+\varepsilon_o)^2 = I_P(1+\varepsilon)^2 \quad \text{for TL,} \tag{14a}$$

$$\bar{I}_P = \frac{I_{Po}}{(1-\varepsilon_o)^2} = I_P \frac{(1+\varepsilon_d)^2}{(1-\varepsilon_o)^2} \quad \text{for UL,} \tag{14b}$$

$$\bar{I}_P = \frac{I_{Po}}{(1-\varepsilon_o)^2} = \frac{I_P}{(1-\varepsilon)^2} \quad \text{for EL.} \tag{14c}$$

(c) *Variations of internal flow velocity of transported fluid*. From the fluid mechanics (Munson et al., 1994), the continuity equation for transitions of a transportation rate among the three states can be displayed in the form

$$\bar{A}_i \bar{V}_i = A_{io}(s_o) V_{io}(s_o) = A_i(s,t) V_i(s,t) + \frac{\partial \forall_{cv}(s,t)}{\partial t}. \tag{15}$$

Nevertheless, because the pipe volume is conserved, time rate of control volume of the pipe $\partial \forall_{cv}/\partial t$ is zero. With application of Eqs. (12), Eq. (15) yields the relationships of internal flow velocities at the three states as follows:

$$\bar{V}_i = \frac{V_{io}}{1+\varepsilon_o} = \frac{V_i}{1+\varepsilon} \quad \text{for TL,} \tag{16a}$$

$$\bar{V}_i = V_{io}(1-\varepsilon_o) = \frac{(1-\varepsilon_o)V_i}{(1+\varepsilon_d)} \quad \text{for UL,} \tag{16b}$$

$$\bar{V}_i = V_{io}(1-\varepsilon_o) = V_i(1-\varepsilon) \quad \text{for EL.} \tag{16c}$$

Physical interpretation of Eqs. (16) substantiates Propositions 1 and 2.

**Proposition 1.** *The plug flow of incompressible fluid inside largely deformable pipes that is* the steady uniform flow ($\partial \bar{V}_i/\partial \alpha = \partial \bar{V}_i/\partial t = 0$) *at the undeformed state*, *would become* the steady nonuniform flow ($\partial V_{io}/\partial \alpha \neq 0$, $\partial V_{io}/\partial t = 0$) *at the equilibrium state*, *and then* the unsteady nonuniform flow ($\partial V_i/\partial \alpha \neq 0$, $\partial V_i/\partial t \neq 0$) *at the displaced state*.

**Proposition 2.** *Extensibility of the pipes causes an increase of internal flow velocity of transported fluid.*

### *2.3. The extensible elastica theory*

A sophisticated strategy highlighted in this work is to adopt the extensible elastica theory for large strain formulations of extensible flexible pipes. In Appendix A, the following extensible elastica theorems corresponding to the three deformation descriptors are developed.

**Theorem 1.** *For the Hookean material pipe, if the TL is employed to describe deformation of the pipe, then the constitutive relations are*

$$\varepsilon_\varsigma = \varepsilon + \varsigma[\kappa(1+\varepsilon) - \bar{\kappa}], \tag{17a}$$

$$N = E\bar{A}_P\varepsilon, \tag{17b}$$

$$M = E\bar{I}_P[\kappa(1+\varepsilon) - \bar{\kappa}], \tag{17c}$$

$$\delta U = \int_{\bar{s}} \{N\delta\varepsilon + M\delta[\kappa(1+\varepsilon) - \bar{\kappa}]\}\, d\bar{s} = \int_{\alpha} [N\delta s' + M\delta(\theta' - \bar{\theta}')]\, d\alpha, \tag{17d}$$

in which $\varepsilon_\varsigma$ is the axial strain at any fibre radius $\varsigma$, $E$ the elastic modulus, $N$ the axial force, $M$ the bending moment, and $U$ the strain energy of the pipe.

**Theorem 2.** *For the Hookean material pipe, if the UL is employed to describe deformation of the pipe, then the constitutive relations are*

$$\varepsilon_\varsigma = \varepsilon + \varsigma[\kappa(1+\varepsilon_d) - \bar{\kappa}(1-\varepsilon_o)], \tag{18a}$$

$$N = EA_{Po}\varepsilon, \tag{18b}$$

$$M = EI_{Po}[\kappa(1+\varepsilon_d) - \bar{\kappa}(1-\varepsilon_o)], \tag{18c}$$

$$\delta U = \int_{\bar{s}} \{N\delta\varepsilon + M\delta[\kappa(1+\varepsilon_d) - \bar{\kappa}(1-\varepsilon_o)]\}\, \mathrm{d}s_o = \int_{\alpha} [N\delta s' + M\delta(\theta' - \bar{\theta}')]\, \mathrm{d}\alpha. \tag{18d}$$

**Theorem 3.** *For the Hookean material pipe, if the EL is employed to describe deformation of the pipe, then the constitutive relations are*

$$\varepsilon_\varsigma = \varepsilon + \varsigma[\kappa - \bar{\kappa}(1-\varepsilon)], \tag{19a}$$

$$N = EA_P\varepsilon, \tag{19b}$$

$$M = EI_P[\kappa - \bar{\kappa}(1-\varepsilon)], \tag{19c}$$

$$\delta U = \int_{s} \{N\delta\varepsilon + M\delta[\kappa - \bar{\kappa}(1-\varepsilon)]\}\, \mathrm{d}s = \int_{\alpha} [N\delta s' + M\delta(\theta' - \bar{\theta}')]\, \mathrm{d}\alpha. \tag{19d}$$

### 2.4. The apparent tension concept

Externally and internally flowing fluids interact with a pipe through hydrostatic and hydrodynamic pressures. The apparent tension concept is proposed herein to represent the effect of hydrostatic pressures, while the effect of dynamic pressures will be considered in the next section.

The apparent tension concept for handling the hydrostatic pressure effect of external and internal fluids is illustrated in Fig. 4. First of all, Archimedes' law, which will be used in the apparent tension concept, is recalled. As shown in Fig. 4(a), equilibrium of an external fluid column in an external pressure field proves physically that the enclosing external pressure field induces a vertical buoyancy force equal to the weight of the external fluid column $\rho_e g \forall_e$. This tenet is commonly referred to as *the first law of Archimedes*. A reverse viewpoint of the first law of Archimedes yields the corollary that the enclosing internal pressure field generates the apparent weight of the internal fluid column $\rho_i g \forall_i$.

It is remarkable that Archimedes' principle is usable with the enclosing pressure fields. However, for marine pipes, the pressure fields of external and internal fluids surround only external and internal side surfaces of the pipe segment, as seen in Fig. 4(b). Both cut ends of the pipe segment are not subjected to the pressure fields, which are called *the missing pressures*. Archimedes' principle cannot therefore be used straightforwardly for marine pipe analysis. Fortunately, this problem can be solved by the superposition technique to transform the real system into the apparent system of marine pipes as follows.

*Step* 1: The total forces acting on *the real system of the pipe column* (the pipe plus transported fluid) as shown in Fig. 4(b) are equal to the summation of the forces acting on the pipe columns in Figs. 4(c–e):

$$\text{Fig. 4(b)} = \text{Fig. 4(c)} + \text{Fig. 4(d)} + \text{Fig. 4(e)}. \tag{20}$$

*Step* 2: The forces acting on the pipe column in Fig. 4(c) are equal to the summation of the forces acting on the pipe columns in Figs. 4(f) and (g):

$$\text{Fig. 4(c)} = \text{Fig. 4(f)} + \text{Fig. 4(g)}. \tag{21}$$

*Step* 3: The static pressures exerted on the pipe column in Fig. 4(f) are made enclosing the pipe column by adding in the missing pressures at both cut ends of the pipe segment. However, the added pressures are nonexistent, so they must be removed for balance by applying the opposite pressure fields at the both ends of the pipe in Fig. 4(g).

*Step* 4: After the pressure fields enclose the pipe segment, Archimedes's principle is now applicable. Therefore, the enclosing external and internal pressure fields induce the buoyancy force $W_e$ and the internal fluid weight $W_i$:

$$W_e = \rho_e \forall_e g, \quad W_i = \rho_i \forall_i g. \tag{22a, b}$$

In addition, the enclosing pressure fields in Fig. 4(f) induce triaxial stresses, which in polar coordinates are: the radial stress $\sigma_r$, the circumferential stress $\sigma_\theta$, and the tensile stress due to the missing pressures $\sigma_t$. These triaxial stresses provoke the axial force

$$T_{\text{tri}} = EA_P\varepsilon_{tri} = (2v-1)(p_eA_e - p_iA_i). \tag{22c}$$

Note that from the theory of elasticity (Timoshenko and Goodier, 1984):

$$\varepsilon_{tri} = [\sigma_t - v(\sigma_r + \sigma_\theta)]/E, \tag{22d}$$

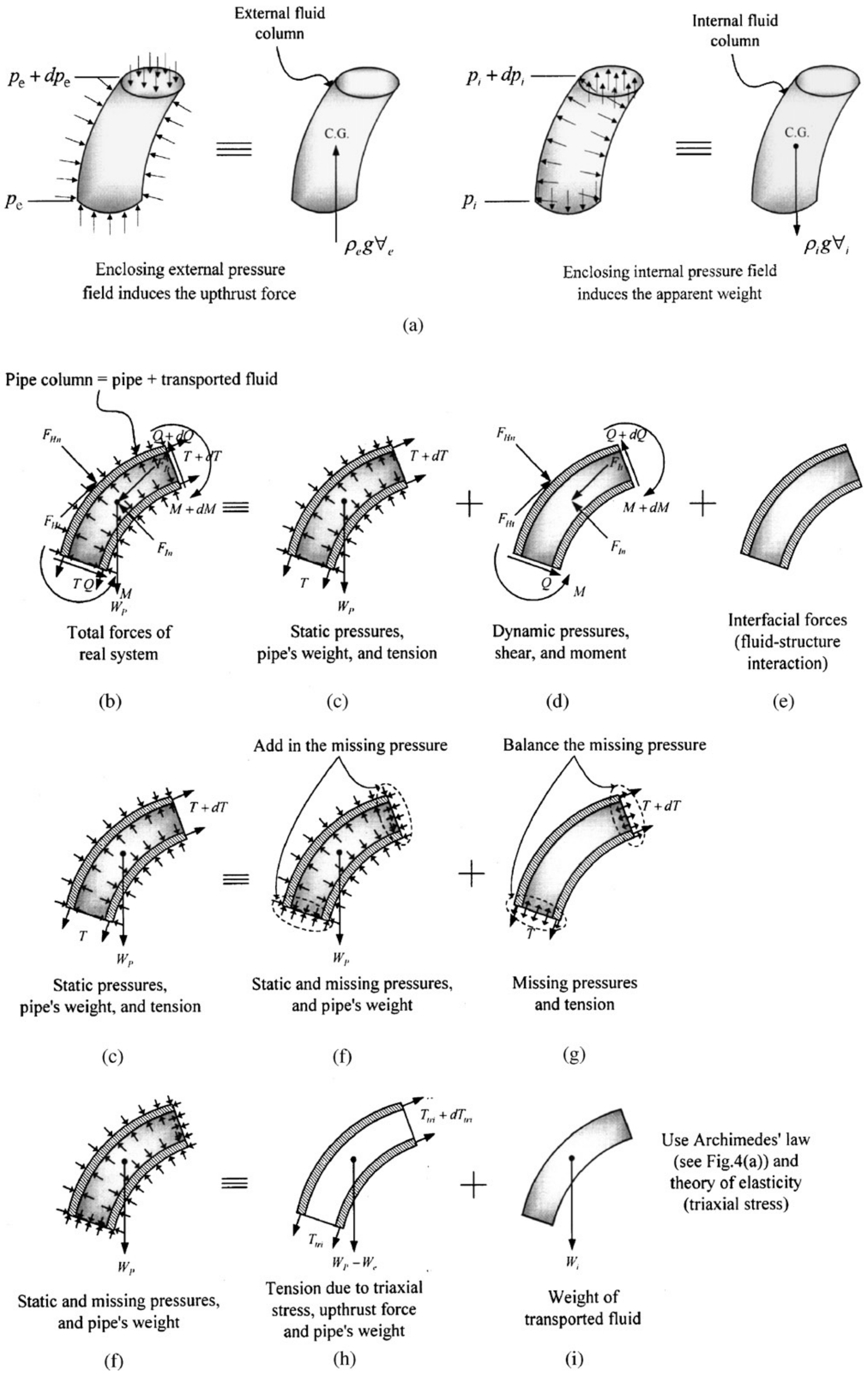


Fig. 4. Transformation from the real system to the apparent system.

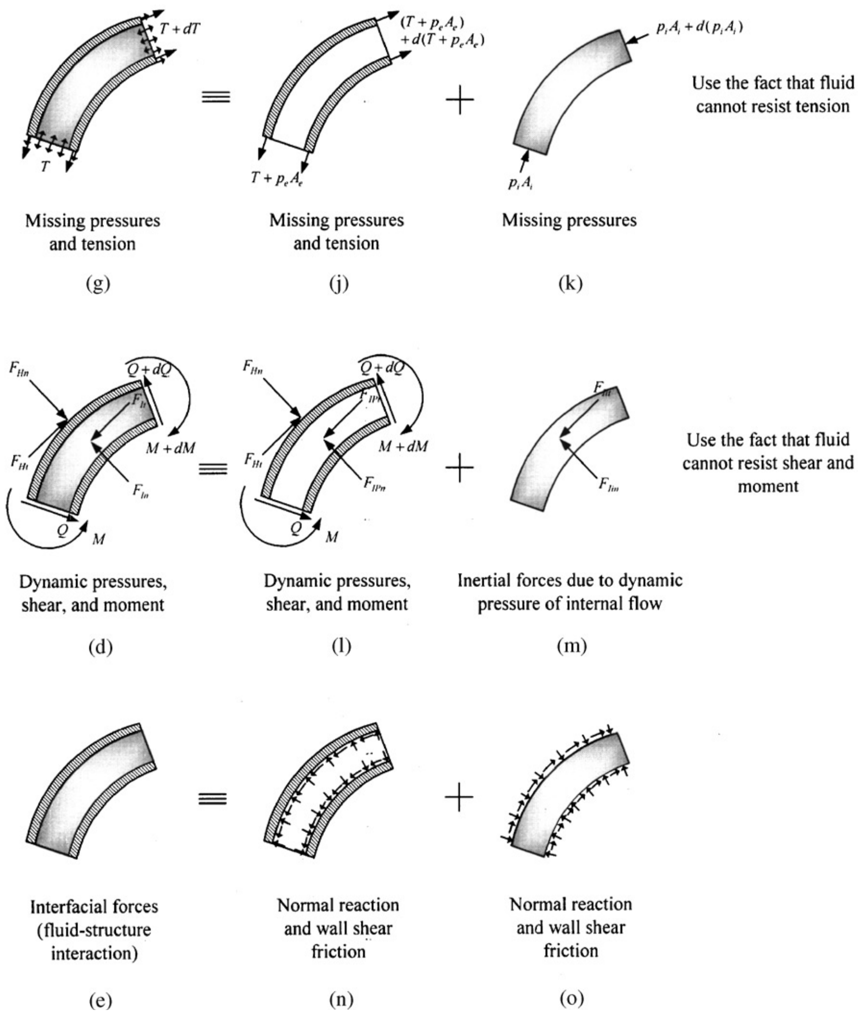


Fig. 4 (*continued*).

and the enclosing pressure fields in Fig. 4(f) yield

$$\sigma_\theta = \sigma_P + \tau, \quad \sigma_r = \sigma_P - \tau, \quad \sigma_\theta + \sigma_r = 2\sigma_P, \tag{22e−g}$$

$$\sigma_P = (p_i A_i - p_e A_e)/A_P, \tag{22h}$$

where $\tau$ is the shear stress in pipe wall, and $\sigma_P$ the end effect stress (Sparks, 1984).

*Step* 5: The pipe column in Fig. 4(f) is decomposed into a combination of the pipe element in Fig. 4(h) and the transported fluid element in Fig. 4(i):

$$\text{Fig. 4(f)} = \text{Fig. 4(h)} + \text{Fig. 4(i)}. \tag{23}$$

The effect of the enclosing pressure fields is replaced by $W_e$ and $T_{\text{tri}}$ in Fig. 4(h), and by $W_i$ in Fig. 4(i).

*Step* 6: The pipe column in Fig. 4(g) is decomposed into a combination of the pipe element in Fig. 4(j) and the transported fluid element in Fig. 4(k):

$$\text{Fig. 4(g)} = \text{Fig. 4(j)} + \text{Fig. 4(k)}. \tag{24}$$

The missing pressure $p_e A_e$ is entirely transmitted to the pipe element, because the transported fluid element cannot resist tension.

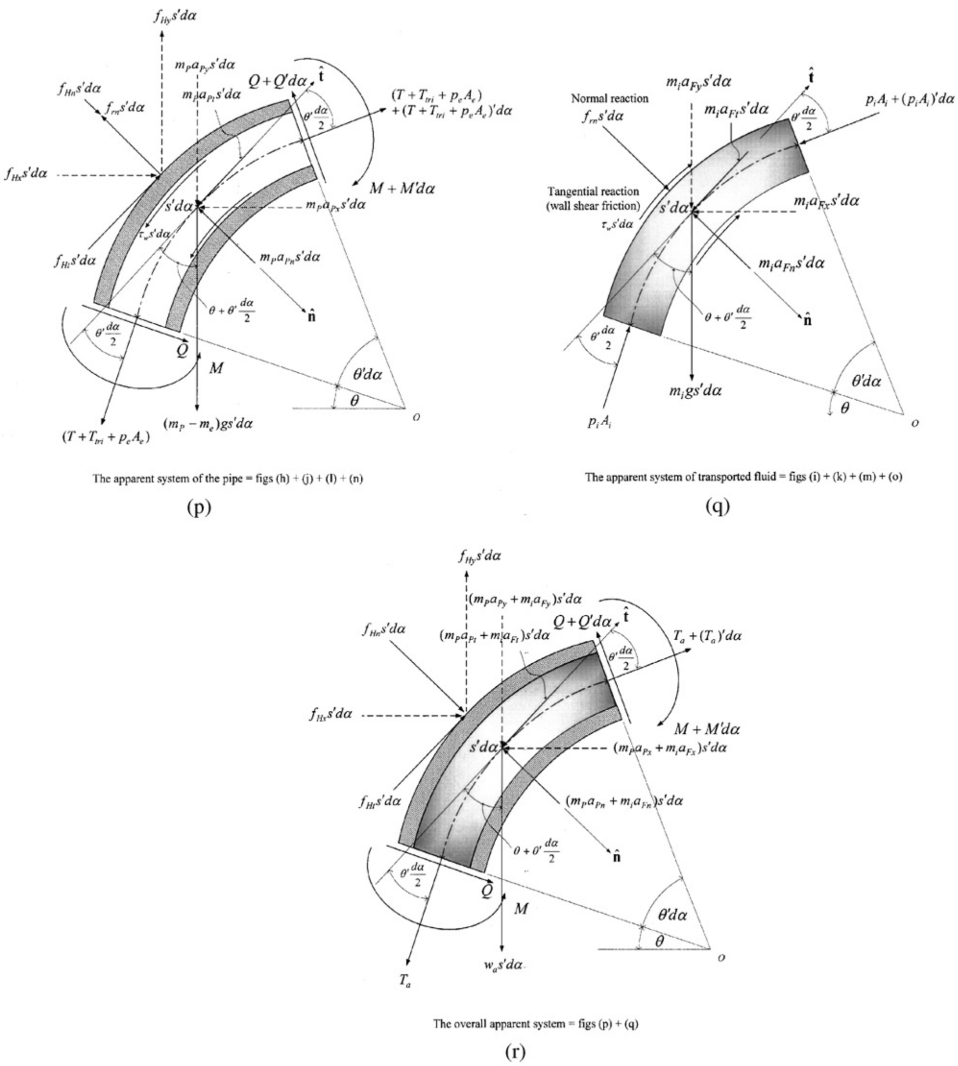


Fig. 4 (*continued*).

*Step* 7: The pipe column in Fig. 4(d) is decomposed into a combination of the pipe element in Fig. 4(l) and the transported fluid element in Fig. 4(m):

$$\text{Fig. 4(d)} = \text{Fig. 4(l)} + \text{Fig. 4(m)}. \tag{25}$$

Shear forces and bending moments are entirely transmitted to the pipe element, because the transported fluid element cannot resist them.

*Step* 8: The pipe column in Fig. 4(e) is decomposed into a combination of the pipe element in Fig. 4(n) and the transported fluid element in Fig. 4(o):

$$\text{Fig. 4(e)} = \text{Fig. 4(n)} + \text{Fig. 4(o)}. \tag{26}$$

*Step* 9: Substituting Eqs. (21), (23)–(26) into Eq. (20) together with some manipulation, one can obtain the expression

$$\text{Fig. 4(b)} = [\text{Fig. 4(h)} + \text{Fig. 4(j)} + \text{Fig. 4(l)} + \text{Fig. 4(n)}] + [\text{Fig. 4(i)} + \text{Fig. 4(k)}\text{Fig. 4(m)} + \text{Fig. 4(o)}]. \tag{27}$$

The first bracket on the right-hand side of Eq. (27) represents the apparent system of the pipe as portrayed in Fig. 4(p), while the second bracket expresses the apparent system of transported fluid as displayed in Fig. 4(q). Combination of the apparent systems of the pipe and transported fluid in Eq. (27) yields the overall apparent system of the pipe column that is subjected to the apparent weight $w_a$ and the apparent tension $T_a$ as shown in Fig. 4(r).

Writing expressions for the apparent weight and the apparent tension generally for the three deformation descriptors, one obtains

$$w_a = (\rho_P \tilde{A}_P - \rho_e \tilde{A}_e + \rho_i \tilde{A}_i)g, \tag{28}$$

$$T_a = E\tilde{A}_P \varepsilon = T + 2v(p_e \tilde{A}_e - p_i \tilde{A}_i), \tag{29}$$

in which $\tilde{A}_\alpha = \bar{A}_\alpha$ for TL, $\tilde{A}_\alpha = A_{\alpha o}$ for UL, $\tilde{A}_\alpha = A_\alpha$ for EL, and the subscript $\alpha \in \{P, e, i\}$.

Ability to transform the real system into the apparent system of the pipe column establishes Proposition 3 that describes the apparent tension concept.

**Proposition 3.** *The real system of the pipe column that is subjected to static external and internal pressures as shown in* Fig. 4(b) *is equivalent to the overall apparent system of the pipe column that is subjected to the apparent weight and the apparent tension as shown in* Fig. 4(r).

On the other hand, the apparent tension may be expressed as

$$T_a = T_e + T_{\mathrm{tri}}, \tag{30}$$

where

$$T_e = T + p_e \tilde{A}_e - p_i \tilde{A}_i \tag{31}$$

is referred to as the effective tension (Sparks, 1984). From Eqs. (29), it is seen that the condition $T_a = T_e$ is achieved if, and only if, $v = 0.5$. This signifies that *the effective tension concept is a subset of the apparent tension concept*, and can be evidently inaccurate, whenever realistic Poisson's ratio of the pipe is significantly different from 0.5.

### 2.5. Dynamic interactions between fluids and pipes

For flexible marine pipes transporting fluid, dynamic interactions between fluid and pipe occur due to steady and unsteady flows of external and internal fluids through the displaced pipe. Steady flows will cause quasi-static forces, and unsteady flows will engender dynamic forces to act on the pipe wall. The flow outside the pipe is normally associated with cross flows of ocean currents and waves, whereas the flow inside the pipe relates to the tangential flow of transported fluid.

#### 2.5.1. Hydrodynamic forces due to cross-flows of currents and waves

Based on the coupled Morison equation (Chakrabarti, 1990), the hydrodynamic forces exerted on flexible marine pipes with large displacements in natural coordinates can be expressed as

$$\mathbf{f}_H = \begin{Bmatrix} f_{Hn} \\ f_{Ht} \end{Bmatrix} = \underbrace{0.5\rho_e D_e \begin{Bmatrix} C_{Dn}\gamma_n|\gamma_n| \\ \pi C_{Dt}\gamma_t|\gamma_t| \end{Bmatrix}}_{\text{Viscous drag force}} + \underbrace{\rho_e A_e C_a \begin{Bmatrix} \dot{\gamma}_n \\ \dot{\gamma}_t \end{Bmatrix}}_{\text{Hydrodynamic mass force}} + \underbrace{\rho_e A_e \begin{Bmatrix} \dot{V}_{Hn} \\ \dot{V}_{Ht} \end{Bmatrix}}_{\text{Froude-Krylov force}}, \tag{32}$$

where overdot denotes $\partial(\,)/\partial t$, $C_{Dn}$ and $C_{Dt}$ are the normal and tangential drag coefficients, $C_a$ the added mass coefficient, $V_{Hn}$ and $V_{Ht}$ the normal and tangential velocities of currents and waves; and $\gamma_n = V_{Hn} - \dot{u}_n$ and $\gamma_t = V_{Ht} - \dot{v}_n$ are the velocities of currents and waves relative to pipe velocities $\dot{u}_n$ and $\dot{v}_n$ in normal and tangential directions, respectively. For large strain consideration, the effect of cross-sectional changes of the pipe according to Eqs. (12) and (13) has to be applied to Eq. (32).

In order to eliminate the difficulty of operating with absolute functions in Eq. (32), the signum function is introduced:

$$\mathrm{sgn}(\gamma) = \begin{cases} 1 & \text{if } \gamma \geq 0, \\ -1 & \text{if } \gamma < 0. \end{cases} \tag{33}$$

Using the signum function, Eq. (32) can be manipulated into the form

$$\mathbf{f}_H = \begin{Bmatrix} f_{Hn} \\ f_{Ht} \end{Bmatrix} = -\underbrace{\begin{bmatrix} C_a^* & 0 \\ 0 & C_a^* \end{bmatrix} \begin{Bmatrix} \ddot{u}_n \\ \ddot{v}_n \end{Bmatrix}}_{\text{Added mass force}} - \underbrace{\begin{bmatrix} C_{eqn}^* & 0 \\ 0 & C_{eqt}^* \end{bmatrix} \begin{Bmatrix} \dot{u}_n \\ \dot{v}_n \end{Bmatrix}}_{\text{Hydrodynamic damping force}} + \underbrace{\begin{Bmatrix} C_{Dn}^* V_{Hn}^2 + C_M^* \dot{V}_{Hn} \\ C_{Dt}^* V_{Ht}^2 + C_M^* \dot{V}_{Ht} \end{Bmatrix}}_{\text{Hydrodynamic excitation}}, \tag{34}$$

where the c oefficients of equivalent damping and drag forces in the normal direction are

$$C_{eqn}^* = C_{Dn}^*[2V_{Hn} - \dot{u}_n],\ C_{Dn}^* = 0.5\rho_e D_e C_{Dn}\, sgn(\gamma_n); \tag{35a, b}$$

the coefficients of equivalent damping and drag forces in the tangential direction are

$$C_{eqt}^* = C_{Dt}^*[2V_{Ht} - \dot{v}_n], \quad C_{Dt}^* = 0.5\rho_e D_e \pi C_{Dt}\, \mathrm{sgn}(\gamma_t); \tag{35c, d}$$

and the coefficients of added mass and inertia forces are

$$C_a^* = \rho_e A_e C_a, \quad C_M^* = \rho_e A_e C_M, \tag{35e, f}$$

in which $C_M = 1 + C_a$ is the inertia coefficient.

In Cartesian coordinates, Eq. (34) can be transformed to

$$\mathbf{f}_H = \begin{Bmatrix} f_{Hx} \\ f_{Hy} \end{Bmatrix} = -\underbrace{\begin{bmatrix} C_a^* & 0 \\ 0 & C_a^* \end{bmatrix} \begin{Bmatrix} \ddot{x} \\ \ddot{y} \end{Bmatrix}}_{\text{Added mass force}} - \underbrace{\begin{bmatrix} C_{eqx}^* & C_{eqxy}^* \\ C_{eqxy}^* & C_{eqy}^* \end{bmatrix} \begin{Bmatrix} \dot{x} \\ \dot{y} \end{Bmatrix}}_{\text{Hydrodynamic damping force}} + \underbrace{\begin{Bmatrix} C_{Dx}^* V_{Hx}^2 + 2C_{Dxy1}^* V_{Hx} V_{Hy} + C_{Dxy2}^* V_{Hy}^2 + C_M^* \dot{V}_{Hx} \\ C_{Dy}^* V_{Hy}^2 + 2C_{Dxy2}^* V_{Hx} V_{Hy} + C_{Dxy1}^* V_{Hx}^2 + C_M^* \dot{V}_{Hy} \end{Bmatrix}}_{\text{Hydrodynamic excitation}}, \tag{36}$$

where $V_{Hx}$ and $V_{Hy}$ are the horizontal and vertical velocities of external fluid; the coefficients of equivalent damping and drag forces in the horizontal direction are

$$C_{eqx}^* = C_{eqn}^* \cos^2\theta + C_{eqt}^* \sin^2\theta, \quad C_{Dx}^* = C_{Dn}^* \cos^3\theta + C_{Dt}^* \sin^3\theta; \tag{37a, b}$$

the coefficients of equivalent damping and drag forces in the vertical direction are

$$C_{eqy}^* = C_{eqn}^* \sin^2\theta + C_{eqt}^* \cos^2\theta, \quad C_{Dy}^* = -C_{Dn}^* \sin^3\theta + C_{Dt}^* \cos^3\theta; \tag{37c, d}$$

the coupling coefficient of equivalent hydrodynamic damping in the $x - y$ plane is

$$C_{eqxy}^* = (-C_{eqn}^* + C_{eqt}^*)\sin\theta\cos\theta; \tag{37e}$$

and the coupling coefficients of drag forces in the $x - y$ plane are

$$C_{Dxy1}^* = -C_{Dn}^* \sin\theta\cos^2\theta + C_{Dt}^* \sin^2\theta\cos\theta, \tag{37f}$$

$$C_{Dxy2}^* = C_{Dn}^* \sin^2\theta\cos\theta + C_{Dt}^* \sin\theta\cos^2\theta. \tag{37g}$$

At the equilibrium state, static loading is due only to the steady flow of external fluid. Therefore, the hydrodynamic forces from Eqs. (34) and (36) are reduced to

$$\mathbf{f}_{Ho} = \begin{Bmatrix} f_{Hno} \\ f_{Hto} \end{Bmatrix} = \begin{Bmatrix} C_{Dno}^* V_{Hno}^2 \\ C_{Dto}^* V_{Hto}^2 \end{Bmatrix}, \tag{38}$$

$$\mathbf{f}_{Ho} = \begin{Bmatrix} f_{Hxo} \\ f_{Hyo} \end{Bmatrix} = \begin{Bmatrix} C_{Dxo}^* V_{Hxo}^2 + 2C_{Dxy1o}^* V_{Hxo} V_{Hyo} + C_{Dxy2o}^* V_{Hyo}^2 \\ C_{Dyo}^* V_{Hyo}^2 + 2C_{Dxy2o}^* V_{Hxo} V_{Hyo} + C_{Dxy1o}^* V_{Hxo}^2 \end{Bmatrix}, \tag{39}$$

respectively. Note that the additional subscripts '$o$' on all variables designate the equilibrium-state parameters. For example, $C_{Dno}^*$ implies the equilibrium state of $C_{Dn}^*$; hence, Eq. (35b) uses equilibrium-state parameters to obtain $C_{Dno}^* = 0.5\rho_e D_{eo} C_{Dn}\, \mathrm{sgn}(\gamma_{no})$.

### 2.5.2. Hydrodynamic forces due to internal flow of transported fluid

Based on the control volume approach of Computational Fluid Dynamics, hydrodynamic forces due to flow of transported fluid inside extensible flexible pipes with large deformation can be derived as follows. Let $\mathbf{V}_F$ and $\mathbf{V}_P$ represent the velocity vectors of transported fluid and the pipe with respect to the fixed frame of reference, then the velocity vector of transported fluid relative to the pipe velocity is given by

$$\mathbf{V}_{FP} = V_{FP}\hat{\mathbf{t}} = V_{FP}\,\partial \mathbf{r}_P/\partial s = \mathbf{V}_F - \mathbf{V}_P, \tag{40}$$

where $V_{FP}$ is the internal flow velocity function: $V_{FP} = \bar{V}_i$, $V_{FP} = V_{io}$, and $V_{FP} = V_i$ at states 1, 2, and 3, respectively.

From Newton's law of momentum conservation, hydrodynamic pressures due to internal flow induces the inertial force on the transported mass:

$$\int_{\forall_i} \mathbf{B}_i \, d\forall_i = \int_{\forall_i} \frac{D(\rho_i \mathbf{V}_F)}{Dt} d\forall_i = \int_{\forall_i} \left[ \frac{D\rho_i}{Dt} \mathbf{V}_F + \rho_i \mathbf{a}_F \right] d\forall_i, \tag{41}$$

where $\mathbf{B}_i$ is the inertial force per unit control volume $\forall_i$, $\mathbf{a}_F$ the acceleration vector of transported fluid with respect to the fixed frame of reference, and

$$\frac{\mathrm{D}()}{\mathrm{D}t} = \frac{\partial()}{\partial t} + (\mathbf{V}_{FP} \cdot \nabla)() = \frac{\partial()}{\partial t} + \frac{V_{FP}}{s'}\frac{\partial()}{\partial \alpha}. \tag{42}$$

Note that

$$\mathbf{V}_{FP}.\nabla = V_{FP}\left[\frac{\partial x}{\partial s}\hat{\mathbf{i}} + \frac{\partial y}{\partial s}\hat{\mathbf{j}} + \frac{\partial z}{\partial s}\hat{\mathbf{k}}\right]\left[\frac{\partial}{\partial x}\hat{\mathbf{i}} + \frac{\partial}{\partial y}\hat{\mathbf{j}} + \frac{\partial}{\partial z}\hat{\mathbf{k}}\right] = V_{FP}\frac{\partial}{\partial s} = \frac{V_{FP}}{s'}\frac{\partial}{\partial \alpha}. \tag{43}$$

Lemma 1 shows that $\mathrm{D}\rho_i/\mathrm{D}t$ vanishes.

**Lemma 1.** *The conservation condition of transported mass yields* $\mathrm{D}\rho_i/\mathrm{D}t = 0$.

**Proof.** Utilizing Eq. (40), Eq. (41) can be written as

$$\int_{\forall_i} \mathbf{B}_i \, d\forall_i = \int_{\forall_i} \left[\frac{\mathrm{D}(\rho_i \mathbf{V}_P)}{\mathrm{D}t}\right] d\forall_i + \int_{\forall_i} \left[\frac{\mathrm{D}(\rho_i \mathbf{V}_{FP})}{\mathrm{D}t}\right] d\forall_i. \tag{44}$$

From the Reynolds transport theorem (Shames, 1992), the last integral is given by

$$\int_{\forall_i} \frac{\mathrm{D}(\rho_i \mathbf{V}_{FP})}{\mathrm{D}t} d\forall_i = \frac{\partial}{\partial t}\left[\int_{\forall_i} (\rho_i \mathbf{V}_{FP})\, d\forall_i\right] + \oiint_{\tilde{A}_{si}} \mathbf{V}_{FP}(\rho_i \mathbf{V}_{FP}\, d\mathbf{A}_{si}), \tag{45}$$

where $\mathbf{A}_{si}$ is the vector of internal control surface of the pipe $\tilde{A}_{si}$.

Employing the Gauss divergence theorem, one can demonstrate that

$$\oiint_{\tilde{A}_i} \mathbf{V}_{FP}(\rho_i \mathbf{V}_{FP} \cdot d\mathbf{A}_{si}) = \int_{\forall_i} \left[(\rho_i \mathbf{V}_{FP} \cdot \nabla)\mathbf{V}_{FP} + \nabla \cdot (\rho_i \mathbf{V}_{FP})\mathbf{V}_{FP}\right] d\forall_i. \tag{46}$$

Substituting Eqs. (46) into Eq. (45) together with some manipulation, one obtains

$$\int_{\forall_i} \frac{\mathrm{D}(\rho_i \mathbf{V}_{FP})}{\mathrm{D}t} d\forall_i = \int_{\forall_i} \left\{ \rho_i \underbrace{\left[\frac{\partial \mathbf{V}_{FP}}{\partial t} + (\mathbf{V}_{FP} \cdot \nabla)\mathbf{V}_{FP}\right]}_{(1)} + \underbrace{\left[\frac{\partial \rho_i}{\partial t} + \nabla \cdot (\rho_i \mathbf{V}_{FP})\right]}_{(2)} \mathbf{V}_{FP} \right\} d\forall_i. \tag{47}$$

Referring to Eq. (42), the bracketed term (1) is known as the acceleration of transported fluid $\mathbf{a}_{FP}$, whereas term (2) is zero due to the continuity condition of conservation of mass. Thereby, Eq. (47) yields

$$\frac{\mathrm{D}(\rho_i \mathbf{V}_{FP})}{\mathrm{D}t} = \rho_i \mathbf{a}_{FP}. \tag{48}$$

Since

$$\frac{\mathrm{D}(\rho_i \mathbf{V}_{FP})}{\mathrm{D}t} = \frac{\mathrm{D}\rho_i}{\mathrm{D}t}\mathbf{V}_{FP} + \rho_i \mathbf{a}_{FP},$$

and $\mathbf{V}_{FP} \neq 0$, Eq. (48) is valid if, and only if,

$$\mathrm{D}\rho_i/\mathrm{D}t = 0. \; \square \tag{49}$$

Using Lemma 1 in Eq. (41), one can constitute Proposition 4.

**Proposition 4.** *Internal flow of transported fluid through the moving, deforming internal control volume of the pipe induces the inertial force exerted on the pipe wall*:

$$\mathbf{B}_i = \rho_i \mathbf{a}_F \quad or \quad \mathbf{F}_i = m_i \mathbf{a}_F, \tag{50a, b}$$

*where* $\mathbf{F}_i$ *and* $m_i$ *are the inertial force and the transported mass per unit length of the pipe.*

From Eqs. (50), it is seen that determining the inertial force on the transported fluid needs the expression of transported mass acceleration $\mathbf{a}_F$. Based on Eulerian mechanics (Huang, 1993), the velocity and acceleration of transported fluid can be derived as

$$\mathbf{V}_F = \mathbf{V}_P + \mathbf{V}_{FP} = \frac{\partial \mathbf{r}_P}{\partial t} + \frac{V_{FP}}{s'}\frac{\partial \mathbf{r}_P}{\partial \alpha}, \tag{51}$$

$$\begin{aligned}\mathbf{a}_F = \mathbf{a}_P + \mathbf{a}_{FP} &= \frac{\mathrm{D}\mathbf{V}_P}{\mathrm{D}t} + \frac{\mathrm{D}\mathbf{V}_{FP}}{\mathrm{D}t} = \frac{\mathrm{D}}{\mathrm{D}t}\left(\frac{\partial \mathbf{r}_P}{\partial t}\right) + \frac{\mathrm{D}}{\mathrm{D}t}\left(\frac{V_{FP}}{s'}\frac{\partial \mathbf{r}_P}{\partial \alpha}\right) \\ &= \underbrace{\left[\frac{\partial^2 \mathbf{r}_P}{\partial t^2} + \frac{V_{FP}}{s'}\frac{\partial^2 \mathbf{r}_P}{\partial \alpha\,\partial t}\right]}_{\mathbf{a}_P} + \underbrace{\frac{V_{FP}}{s'}\left[\frac{\partial^2 \mathbf{r}_P}{\partial \alpha\,\partial t} + \frac{V_{FP}}{s'}\frac{\partial^2 \mathbf{r}_P}{\partial \alpha^2}\right] + \left[\frac{\partial}{\partial t}\left(\frac{V_{FP}}{s'}\right) + \frac{V_{FP}}{s'}\frac{\partial}{\partial \alpha}\left(\frac{V_{FP}}{s'}\right)\right]\frac{\partial \mathbf{r}_P}{\partial \alpha}}_{\mathbf{a}_{FP}}.\end{aligned} \tag{52}$$

Eq. (52) can be rearranged to obtain

$$\mathbf{a}_F = \underbrace{\frac{\partial^2 \mathbf{r}_P}{\partial t^2}}_{(1)} + \underbrace{\left(\frac{2V_{FP}}{s'}\right)\frac{\partial^2 \mathbf{r}_P}{\partial \alpha\,\partial t}}_{(2)} + \underbrace{\left(\frac{V_{FP}}{s'}\right)^2\frac{\partial^2 \mathbf{r}_P}{\partial \alpha^2}}_{(3)} + \left[\underbrace{\frac{\dot{V}_{FP}}{s'}}_{(4)} + \underbrace{\frac{V_{FP}V'_{FP}}{s'^2}}_{(5)} \underbrace{- \frac{V_{FP}\dot{s}'}{s'^2} - \frac{V_{FP}^2 s''}{s'^3}}_{(6)}\right]\frac{\partial \mathbf{r}_P}{\partial \alpha}, \tag{53}$$

in which term (1) is the transported mass acceleration, (2) the coriolis acceleration, (3) the centripetal acceleration, (4) the local acceleration due to unsteady flow, (5) the convective acceleration due to nonuniform flow, and (6) the relative accelerations due to local coordinate rotation and displacement.

In 2-D Cartesian coordinates, at the displaced state:

$$V_{FP} = V_i,\ \ \mathbf{r}_P = x\hat{\mathbf{i}} + y\hat{\mathbf{j}},\ \ s' = \sqrt{x'^2 + y'^2},\ \ s's'' = x'x'' + y'y'',\ \ s'\dot{s}' = x'\dot{x}' + y'\dot{y}'. \tag{54a–e}$$

Inserting Eqs. (54) into Eqs. (51) and (53), one obtains

$$\mathbf{V}_F = [\dot{x} + V_i x'/s']\hat{\mathbf{i}} + [\dot{y} + V_i y'/s']\hat{\mathbf{j}}, \tag{55}$$

$$\begin{aligned}\mathbf{a}_F = &\left\{\ddot{x} + \left[\left(\frac{2}{s'} - \frac{x'^2}{s'^3}\right)\dot{x}' - \left(\frac{x'y'}{s'^3}\right)\dot{y}'\right]V_i + \left(\frac{\kappa y'}{s'}\right)V_i^2 + \left(\frac{DV_i}{Dt}\right)\frac{x'}{s'}\right\}\hat{\mathbf{i}} \\ &+ \left\{\ddot{y} + \left[-\left(\frac{x'y'}{s'^3}\right)\dot{x}' + \left(\frac{2}{s'} - \frac{y'^2}{s'^3}\right)\dot{y}'\right]V_i - \left(\frac{\kappa x'}{s'}\right)V_i^2 + \left(\frac{DV_i}{Dt}\right)\frac{y'}{s'}\right\}\hat{\mathbf{j}}.\end{aligned} \tag{56}$$

Note that

$$\frac{\kappa y'}{s'} = \left(\frac{y'^2}{s'^4}\right)x'' - \left(\frac{x'y'}{s'^4}\right)y'', \quad -\frac{\kappa x'}{s'} = -\left(\frac{x'y'}{s'^4}\right)x'' + \left(\frac{x'^2}{s'^4}\right)y''. \tag{57a, b}$$

In 2-D natural coordinates, at the displaced state:

$$V_{FP} = V_i, \tag{58a}$$

$$\frac{\partial \mathbf{r}_P}{\partial \alpha} = s'\hat{\mathbf{t}}, \tag{58b}$$

$$\frac{\partial^2 \mathbf{r}_P}{\partial \alpha^2} = s'\theta'\hat{\mathbf{n}} + s''\hat{\mathbf{t}}, \tag{58c}$$

$$\frac{\partial^2 \mathbf{r}_P}{\partial t^2} = \ddot{u}_n\hat{\mathbf{n}} + \ddot{v}_n\hat{\mathbf{t}}, \tag{58d}$$

$$\frac{\partial^2 \mathbf{r}_P}{\partial\alpha\,\partial t} = s'\dot{\theta}\hat{\mathbf{n}} + \dot{s}'\hat{\mathbf{t}}. \tag{58e}$$

Exploiting Eqs. (58), Eqs. (51) and (53) yield

$$\mathbf{V}_F = \dot{u}_n\hat{\mathbf{n}} + (\dot{v}_n + V_i)\hat{\mathbf{t}}, \tag{59}$$

$$\mathbf{a}_F = \left[\ddot{u}_n + 2V_i\dot{\theta} + \kappa V_i^2\right]\hat{\mathbf{n}} + \left[\ddot{v}_n + \frac{V_i\dot{s}'}{s'} + \frac{\mathrm{D}V_i}{\mathrm{D}t}\right]\hat{\mathbf{t}}. \tag{60}$$

It is evident that the relative accelerations due to local coordinate rotation and displacement vanish in the natural system.

At the equilibrium state, $V_{FP} = V_{io}$, $(x, y) = (x_o, y_o)$, $u_n = v_n = 0$, $(s, \theta) = (s_o, \theta_o)$, and the time-dependent terms vanish. Thereby, Eqs. (55), (56), (59), and (60) are reduced to

$$\mathbf{V}_{Fo} = (V_{io}x'_o/s'_o)\hat{\mathbf{i}} + (V_{io}y'_o/s'_o)\hat{\mathbf{j}} = V_{io}\hat{\mathbf{t}}, \tag{61}$$

$$\mathbf{a}_{Fo} = \left\{\left(\frac{\kappa_o y'_o}{s'_o}\right)V_{io}^2 + \frac{V_{io}V'_{io}}{s'_o}\frac{x'_o}{s'_o}\right\}\hat{\mathbf{i}} + \left\{-\left(\frac{\kappa_o x'_o}{s'_o}\right)V_{io}^2 + \frac{V_{io}V'_{io}}{s'_o}\frac{y'_o}{s'_o}\right\}\hat{\mathbf{j}} = \left[\kappa_o V_{io}^2\right]\hat{\mathbf{n}} + \left[\frac{V_{io}V'_{io}}{s'_o}\right]\hat{\mathbf{t}}. \tag{62}$$

## 3. Virtual work formulations

Based on the method of virtual work, the fundamentals of large strain modelling proposed in Section 2 are employed to develop large strain formulations of extensible flexible marine pipes transporting fluid as follows.

*Step* 1: Converting the real system into the apparent system of the marine pipe by the apparent tension concept (Section 2.4).

*Step* 2: Applying the extensible elastica theory (Section 2.3) on the apparent system to obtain the stiffness or internal virtual work equation.

*Step* 3: Expressing the equation of external virtual work induced by the apparent weight (Section 2.4), hydrodynamic forces due to external and internal flows (Section 2.5), and inertial forces of the pipe.

*Step* 4: Applying the principle of virtual work to generate weak and strong forms of the large strain formulations of the apparent system.

### *3.1. Step 2: Applying the extensible elastica theory on the apparent system*

In Fig. 4(r), the overall apparent system is subjected to the apparent tension $T_a$ in place of the axial force $N$ of the real system. Therefore, applying Eqs. (17d), (18d), and (19d) of the extensible elastica theory on the apparent system yields the stiffness equation:

$$\delta U_a = \int_\alpha [T_a\delta s' + M\delta(\theta' - \bar{\theta}')]\,\mathrm{d}\alpha, \tag{63}$$

where $U_a$ is the strain energy of the apparent system,

$$T_a = E\tilde{A}_P\varepsilon, \tag{64a}$$

$$M = \begin{cases} E\bar{I}_P[\kappa(1+\varepsilon) - \bar{\kappa}] & \text{for TL,} \\ EI_{Po}[\kappa(1+\varepsilon_d) - \bar{\kappa}(1-\varepsilon_o)] & \text{for UL,} \\ EI_P[\kappa - \bar{\kappa}(1-\varepsilon)] & \text{for EL.} \end{cases} \tag{64b}$$

From the assumption that the pipe is straight in the undeformed state, and the basic formulas of differential geometry, one has

$$\bar{\kappa} = \bar{\theta}' = 0, \tag{65a}$$

$$\mathrm{s}' = \mathrm{x}' + y', \tag{65b}$$

$$\theta' = (x''y' - x'y'')/s'^2. \tag{65c}$$

Substituting Eq. (65a) into Eq. (64b), and taking the first variation of Eqs. (65b) and (65c) in association with the coordinate transformations of the displacement vectors, one obtains

$$M = B\kappa, \quad B = \begin{cases} E\bar{I}_P(1+\varepsilon) & \textit{for TL}, \\ EI_{Po}(1+\varepsilon_d) & \textit{for UL}, \\ EI_P & \textit{for EL}, \end{cases} \tag{66a, b}$$

in Cartesian coordinates:

$$\delta s' = \left(\frac{x'}{s'}\right)\delta u' + \left(\frac{y'}{s'}\right)\delta v', \tag{67a}$$

$$\delta\theta' = \frac{1}{s'}\left(\frac{y'}{s'}\right)\delta u'' - \left[\kappa\left(\frac{x'}{s'}\right) + \frac{s''}{s'^2}\left(\frac{y'}{s'}\right)\right]\delta u' - \frac{1}{s'}\left(\frac{x'}{s'}\right)\delta v'' - \left[\kappa\left(\frac{y'}{s'}\right) - \frac{s''}{s'^2}\left(\frac{x'}{s'}\right)\right]\delta v', \tag{67b}$$

in natural coordinates:

$$\delta s' = \delta v_n' - \theta'\delta u_n, \tag{68a}$$

$$\delta\theta' = \frac{\partial}{\partial\alpha}\left[\frac{\delta u_n' + \theta'\delta v_n}{s'}\right]. \tag{68b}$$

By substituting Eqs. (66)–(68) into Eq. (63), and then taking integrations by parts twice, the three forms of the internal virtual work can be expressed as follows:

Form 1: In Cartesian coordinates:

$$\delta U_a = \int_\alpha \left\{ \begin{array}{l} \dfrac{B\kappa}{s'}\left(\dfrac{y'}{s'}\right)\delta u'' + \left[(T_a - B\kappa^2)\left(\dfrac{x'}{s'}\right) - B\kappa\dfrac{s''}{s'^2}\left(\dfrac{y'}{s'}\right)\right]\delta u' \\ -\dfrac{B\kappa}{s'}\left(\dfrac{x'}{s'}\right)\delta v'' + \left[(T_a - B\kappa^2)\left(\dfrac{y'}{s'}\right) + B\kappa\dfrac{s''}{s'^2}\left(\dfrac{x'}{s'}\right)\right]\delta v' \end{array} \right\} \mathrm{d}\alpha, \tag{69a}$$

and in natural coordinates:

$$\delta U_a = \int_\alpha \left\{\left[-T_a\theta'\right]\delta u_n + [T_a]\,\delta v_n' + [M]\delta\theta'\right\}\mathrm{d}\alpha. \tag{69b}$$

Form 2 (after a first integration by parts): In Cartesian coordinates:

$$\delta U_a = [M\,\delta\theta]_{\alpha_o}^{\alpha_t} + \int_\alpha \{H\,\delta u' + V\,\delta v'\}\,\mathrm{d}\alpha, \tag{70a}$$

and in natural coordinates:

$$\delta U_a = [M\,\delta\theta]_{\alpha_o}^{\alpha_t} + \int_\alpha \{-[Q]\,\delta u_n' - [T_a\theta']\,\delta u_n + [T_a]\,\delta v_n' + [Q\theta']\,\delta v_n\}\,\mathrm{d}\alpha, \tag{70b}$$

where

$$H = T_a\left(\frac{x'}{s'}\right) - Q\left(\frac{y'}{s'}\right), \tag{71a}$$

$$V = T_a\left(\frac{y'}{s'}\right) + Q\left(\frac{x'}{s'}\right), \tag{71b}$$

$$Q = \frac{M'}{s'} = \frac{(B\kappa)'}{s'}. \tag{71c}$$

Form 3 (after a second integration by parts): In Cartesian coordinates:

$$\delta U_a = [H\,\delta u + V\,\delta v + M\,\delta\theta]_{\alpha_o}^{\alpha_t} + \int_\alpha \{[-H']\delta u + [-V']\delta v\}\,\mathrm{d}\alpha, \tag{72a}$$

and in natural coordinates:

$$\delta U_a = [T_a\,\delta v_n - Q\,\delta u_n + M\,\delta\theta]_{\alpha_o}^{\alpha_t} + \int_\alpha \{[Q' - T_a\theta']\,\delta u_n + [-T_a' - Q\theta']\,\delta v_n\}\,\mathrm{d}\alpha. \tag{72b}$$

Note that

$$x'/s' = \sin\theta, \quad y'/s' = \cos\theta, \quad \kappa = \theta'/s' = (x''y' - x'y'')/s'^3.$$

### 3.2. Step 3: Expressing the equation of external virtual work

The equation of external virtual work is given by

$$\delta W_a = \delta W_w + \delta W_H + \delta W_I, \tag{73}$$

where $W_w$, $W_H$, and $W_I$ are the virtual works done by the apparent weight, hydrodynamic pressures, and inertial forces of the pipe and transported fluid. In Cartesian coordinates:

$$\delta W_w = -\int_\alpha w_a s' \, \delta v \, \mathrm{d}\alpha, \tag{74a}$$

$$\delta W_H = \int_\alpha \left[(f_{Hx}s')\,\delta u + (f_{Hy}s')\delta v\right] \mathrm{d}\alpha, \tag{75a}$$

$$\delta W_I = -\int_\alpha \left[(m_P a_{Px} + m_i a_{Fx})s'\,\delta u + (m_P a_{Py} + m_i a_{Fy})s'\,\delta v\right] \mathrm{d}\alpha. \tag{76a}$$

In natural coordinates:

$$\delta W_w = -\int_\alpha [(-w_a s' \sin\theta)\,\delta u_n + (w_a s' \cos\theta)\,\delta v_n]\, d\alpha, \tag{74b}$$

$$\delta W_H = \int_\alpha \left[(f_{Hn}s')\,\delta u_n + (f_{Ht}s')\,\delta v_n\right] \mathrm{d}\alpha, \tag{75b}$$

$$\delta W_I = -\int_\alpha \left[(m_P a_{Pn} + m_i a_{Fn})s'\,\delta u_n + (m_P a_{Pt} + m_i a_{Ft})s'\,\delta v_n\right] \mathrm{d}\alpha. \tag{76b}$$

Note that $\mathbf{a}_P = a_{Px}\hat{\mathbf{i}} + a_{Py}\hat{\mathbf{j}} = \ddot{\mathbf{r}}_P = \ddot{x}\hat{\mathbf{i}} + \ddot{y}\hat{\mathbf{j}} = \ddot{u}\hat{\mathbf{i}} + \ddot{v}\hat{\mathbf{j}}$ and $\mathbf{a}_P = a_{Pn}\hat{\mathbf{n}} + a_{Pt}\hat{\mathbf{t}} = \ddot{u}_n\hat{\mathbf{n}} + \ddot{v}_n\hat{\mathbf{t}}$. The expressions of $w_a$, $\mathbf{f}_H = f_{Hn}\hat{\mathbf{n}} + f_{Ht}\hat{\mathbf{t}}$, $\mathbf{f}_H = f_{Hx}\hat{\mathbf{i}} + f_{Hy}\hat{\mathbf{j}}$, $\mathbf{a}_F = a_{Fx}\hat{\mathbf{i}} + a_{Fy}\hat{\mathbf{j}}$, and $\mathbf{a}_F = a_{Fn}\hat{\mathbf{n}} + a_{Ft}\hat{\mathbf{t}}$ are given by Eqs. (28), (34), (36), (56), and (60), respectively.

Substituting Eqs. (74)–(76) into Eq. (73), in Cartesian coordinates one obtains

$$\begin{aligned}\delta W_a = &\int_\alpha \left\{s'[f_{Hx} - m_P a_{Px} - m_i a_{Fx}]\,\delta u\right\} \mathrm{d}\alpha \\ &+ \int_\alpha \left\{s'[-w_a + f_{Hy} - m_P a_{Py} - m_i a_{Fy}]\,\delta v\right\} \mathrm{d}\alpha,\end{aligned} \tag{77a}$$

and in natural coordinates:

$$\begin{aligned}\delta W_a = &\int_\alpha \left\{s'[w_a \sin\theta + f_{Hn} - m_P a_{Pn} - m_i a_{Fn}]\,\delta u_n\right\} \mathrm{d}\alpha \\ &+ \int_\alpha \left\{s'[-w_a \cos\theta + f_{Ht} - m_P a_{Pt} - m_i a_{Ft}]\,\delta v_n\right\} \mathrm{d}\alpha.\end{aligned} \tag{77b}$$

### 3.3. Step 4: Applying the principle of virtual work

From the principle of virtual work, the total virtual work of the apparent system is zero:

$$\delta\pi_a = \delta U_a - \delta W_a = 0. \tag{78}$$

By substituting Eq. (69), (70), (72), and (77) into Eq. (78), the three weak forms of the total virtual work are obtained as follows:

*Weak form* 1: In Cartesian coordinates:

$$\delta\pi_a = \int_\alpha \left\{ \frac{B\kappa}{s'}\left(\frac{y'}{s'}\right)\delta u'' + \left[(T_a - B\kappa^2)\left(\frac{x'}{s'}\right) - B\kappa\frac{s''}{s'^2}\left(\frac{y'}{s'}\right)\right]\delta u' - s'[f_{Hx} - m_P a_{Px} - m_i a_{Fx}]\,\delta u \right\} \mathrm{d}\alpha$$
$$+ \int_\alpha \left\{ -\frac{B\kappa}{s'}\left(\frac{x'}{s'}\right)\delta v'' + \left[(T_a - B\kappa^2)\left(\frac{y'}{s'}\right) + B\kappa\frac{s''}{s'^2}\left(\frac{x'}{s'}\right)\right]\delta v' - s'[-w_a + f_{Hy} - m_P a_{Py} - m_i a_{Fy}]\,\delta v \right\} \mathrm{d}\alpha = 0. \quad (79a)$$

In natural coordinates:

$$\delta\pi_a = \int_\alpha \{-T_a\theta' - s'[w_a \sin\theta + f_{Hn} - m_P a_{Pn} - m_i a_{Fn}]\}\,\delta u_n\,\mathrm{d}\alpha$$
$$+ \int_\alpha \{[T_a]\,\delta v_n' - s'[-w_a\cos\theta + f_{Ht} - m_P a_{Pt} - m_i a_{Ft}]\,\delta v_n\}\,\mathrm{d}\alpha$$
$$+ \int_\alpha \{[M]\,\delta\theta'\}\,\mathrm{d}\alpha = 0. \quad (79b)$$

*Weak form* 2: In Cartesian coordinates:

$$\delta\pi_a = [M\,\delta\theta]_{\alpha_o}^{\alpha_t} + \int_\alpha \{H\delta u' - s'[f_{Hx} - m_P a_{Px} - m_i a_{Fx}]\,\delta u\}\,\mathrm{d}\alpha$$
$$+ \int_\alpha \{V\delta v' - s'[-w_a + f_{Hy} - m_P a_{Py} - m_i a_{Fy}]\delta v\}\,\mathrm{d}\alpha = 0. \quad (80a)$$

In natural coordinates:

$$\delta\pi_a = [M\,\delta\theta]_{\alpha_o}^{\alpha_t} + \int_\alpha \{-Q\,\delta u_n' - [T_a\theta' + s'(w_a\sin\theta + f_{Hn} - m_P a_{Pn} - m_i a_{Fn})]\,\delta u_n\}\,\mathrm{d}\alpha$$
$$+ \int_\alpha \{T_a\delta v_n' + [Q\theta' - s'(-w_a\cos\theta + f_{Ht} - m_P a_{Pt} - m_i a_{Ft})]\delta v_n\}\,\mathrm{d}\alpha = 0. \quad (80b)$$

*Weak form* 3: In Cartesian coordinates:

$$\delta\pi_a = [H\,\delta u + V\,\delta v + M\,\delta\theta]_{\alpha_o}^{\alpha_t} + \int_\alpha \{[-H' - s'(f_{Hx} - m_P a_{Px} - m_i a_{Fx})]\,\delta u\}\,\mathrm{d}\alpha$$
$$+ \int_\alpha \{[-V' - s'(-w_a + f_{Hy} - m_P a_{Py} - m_i a_{Fy})]\,\delta v\}\,\mathrm{d}\alpha = 0. \quad (81a)$$

In natural coordinates:

$$\delta\pi_a = [T_a\delta v_n - Q\,\delta u_n + M\,\delta\theta]_{\alpha_o}^{\alpha_t}$$
$$+ \int_\alpha \{[Q' - T_a\theta' - s'(w_a\sin\theta + f_{Hn} - m_P a_{Pn} - m_i a_{Fn})]\,\delta u_n\}\,\mathrm{d}\alpha$$
$$+ \int_\alpha \{[-T_a' - Q\theta' - s'(-w_a\cos\theta + f_{Ht} - m_P a_{Pt} - m_i a_{Ft})]\,\delta v_n\}\,\mathrm{d}\alpha = 0. \quad (81b)$$

### *3.3.1. Governing equations by weak form 1*

In view of Eqs. (79), the following conditions are necessary and sufficient for $\delta\pi_a$ to vanish for all admissible functions of virtual displacements.

In Cartesian coordinates:

$$\delta\pi_{ax} = 0: \int_\alpha \left\{ \frac{B\kappa}{s'}\left(\frac{y'}{s'}\right)\delta u'' + \left[(T_a - B\kappa^2)\left(\frac{x'}{s'}\right) - B\kappa\frac{s''}{s'^2}\left(\frac{y'}{s'}\right)\right]\delta u' - s'[f_{Hx} - m_P a_{Px} - m_i a_{Fx}]\,\delta u \right\} \mathrm{d}\alpha = 0, \quad (82)$$

$$\delta\pi_{ay} = 0: \int_\alpha \left\{ -\frac{B\kappa}{s'}\left(\frac{x'}{s'}\right)\delta v'' + \left[(T_a - B\kappa^2)\left(\frac{y'}{s'}\right) + B\kappa\frac{s''}{s'^2}\left(\frac{x'}{s'}\right)\right]\delta v' - s'[-w_a + f_{Hy} - m_P a_{Py} - m_i a_{Fy}]\,\delta v \right\} \mathrm{d}\alpha = 0. \quad (83)$$

In natural coordinates:

$$\delta\pi_{an} = 0 : \int_\alpha \left\{ \left[\frac{B\kappa}{s'}\right] \delta u_n'' - \left[B\kappa \frac{s''}{s'^2}\right] \delta u_n' + [-T_a\theta' - s'(w_a \sin\theta + f_{Hn} - m_P a_{Pn} - m_i a_{Fn})]\, \delta u_n \right\} \mathrm{d}\alpha = 0, \tag{84}$$

$$\delta\pi_{at} = 0 : \int_\alpha \left\{ \left[T_a + B\kappa^2\right] \delta v_n' + \left[\frac{B\kappa}{s'}(\theta'' - \kappa s'') - s'(-w_a \cos\theta + f_{Ht} - m_P a_{Pt} - m_i a_{Ft})\right] \delta v_n \right\} \mathrm{d}\alpha = 0. \tag{85}$$

*3.3.2. Governing equations by weak form 2*

Similarly, in view of Eqs. (80), the following conditions have to be valid.

In Cartesian coordinates:

$$\delta\pi_{ax} = 0 : \int_\alpha \{H\delta u' - s'[f_{Hx} - m_P a_{Px} - m_i a_{Fx}]\, \delta u\} \,\mathrm{d}\alpha = 0, \tag{86}$$

$$\delta\pi_{ay} = 0 : \int_\alpha \{V\delta v' - s'[-w_a + f_{Hy} - m_P a_{Py} - m_i a_{Fy}]\, \delta v\} \,\mathrm{d}\alpha = 0, \tag{87}$$

with the natural boundary condition of bending moment:

$$[M\, \delta\theta]_{\alpha_o}^{\alpha_t} = 0. \tag{88}$$

In natural coordinates:

$$\delta\pi_{an} = 0 : \int_\alpha \{-Q\delta u_n' - [T_a\theta' + s'(w_a \sin\theta + f_{Hn} - m_P a_{Pn} - m_i a_{Fn})]\, \delta u_n\} \,\mathrm{d}\alpha = 0, \tag{89}$$

$$\delta\pi_{at} = 0 : \int_\alpha \{T_a\delta v_n' + [Q\theta' - s'(-w_a\cos\theta + f_{Ht} - m_P a_{Pt} - m_i a_{Ft})]\, \delta v_n\} \,\mathrm{d}\alpha = 0, \tag{90}$$

with the same boundary condition as Eq. (88).

*3.3.3. Governing equations by weak form 3*

Likewise, the necessary and sufficient conditions of Eqs. (81) yield the weak form 3.

In Cartesian coordinates:

$$\delta\pi_{ax} = 0 : \int_\alpha \{[-H' - s'(f_{Hx} - m_P a_{Px} - m_i a_{Fx})]\, \delta u\} \,\mathrm{d}\alpha = 0, \tag{91}$$

$$\delta\pi_{ay} = 0 : \int_\alpha \{[-V' - s'(-w_a + f_{Hy} - m_P a_{Py} - m_i a_{Fy})]\, \delta v\} \,\mathrm{d}\alpha = 0, \tag{92}$$

with the natural boundary conditions of horizontal and vertical forces, and bending moment:

$$[H\, \delta u + V\, \delta v + M\, \delta\theta]_{\alpha_o}^{\alpha_t} = 0. \tag{93}$$

In natural coordinates:

$$\delta\pi_{an} = 0 : \int_\alpha \{[Q' - T_a\theta' - s'(w_a \sin\theta + f_{Hn} - m_P a_{Pn} - m_i a_{Fn})]\, \delta u_n\} \,\mathrm{d}\alpha = 0, \tag{94}$$

$$\delta\pi_{at} = 0 : \int_\alpha \{[-T_a' - Q\theta' - s'(-w_a \cos\theta + f_{Ht} - m_P a_{Pt} - m_i a_{Ft})]\, \delta v_n\} \,\mathrm{d}\alpha = 0, \tag{95}$$

with the natural boundary conditions of apparent tension, shear force, and bending moment:

$$[T_a\, \delta v_n - Q\, \delta u_n + M\, \delta\theta]_{\alpha_o}^{\alpha_t} = 0. \tag{96}$$

It is important to make a decision which forms of governing equations should be used. In the governing equations by weak form 1, there is no natural boundary condition (BC). So if those equations are employed, all natural BCs may be unconstrained. Another choice is using the governing equations by weak form 2 such that all essential BCs and some natural BCs such as Eq. (88) would have to be constrained. On the other hand, if the governing equations by weak form 3 are selected, all essential BCs and all natural BCs such as Eqs. (93) and (96) need to be constrained.

*3.3.4. Strong formulations by weak form 3*

By considering that all virtual displacements $\delta u$, $\delta v$, $\delta u_n$ and $\delta v_n$ in Eqs. (91), (92), (94) and (95) are nonzero, the following strong formulations are achieved:

(i) *Force-based strong form*. In Cartesian coordinates:

$$\Sigma F_x = 0 : -H' - s'(f_{Hx} - m_P a_{Px} - m_i a_{Fx}) = 0, \tag{97}$$

$$\Sigma F_y = 0 : -V' - s'(-w_a + f_{Hy} - m_P a_{Py} - m_i a_{Fy}) = 0. \tag{98}$$

In natural coordinates:

$$\Sigma F_n = 0 : Q' - T_a\theta' - s'(w_a \sin\theta + f_{Hn} - m_P a_{Pn} - m_i a_{Fn}) = 0, \tag{99}$$

$$\Sigma F_t = 0 : -T_a' - Q\theta' - s'(-w_a \cos\theta + f_{Ht} - m_P a_{Pt} - m_i a_{Ft}) = 0. \tag{100}$$

If the right-hand sides of Eqs. (97)–(100) are considered as the residuals, one can demonstrate that based on the Galerkin method, Eqs. (91), (92), (94) and (95) yield the weighted residual forms of Eqs. (97)–(100), respectively. This fact indicates that the governing equations obtained from the weak variational method and the Galerkin residual method, are the same. As a result, if both methods used the same approximating functions, their solutions would be identical.

The vector expressions of Eqs. (97)–(100) are given by

$$-\mathbf{P}' - s'(-w_a\hat{\mathbf{j}} + \mathbf{f}_H - m_P\mathbf{a}_P - m_i\mathbf{a}_F) = 0, \tag{101}$$

where the internal force vectors $\mathbf{P}$ are represented by

$$\mathbf{P}'_{XY} = \begin{Bmatrix} H' \\ V' \end{Bmatrix} \quad \text{and} \quad \mathbf{P}'_{NT} = \begin{Bmatrix} T_a\theta' - Q' \\ T_a' + Q\theta' \end{Bmatrix} = \begin{bmatrix} y'/s' & -x'/s' \\ x'/s' & y'/s' \end{bmatrix} \begin{Bmatrix} H' \\ V' \end{Bmatrix}, \tag{102}$$

in Cartesian and natural coordinate systems, respectively.

(ii) *Displacement-based strong form.* Based on Eqs. (71a)–(71c), one can demonstrate that

$$H = \left[(T_a - B\kappa^2)\frac{x'}{s'} - B\kappa\left(\frac{s''}{s'^2}\right)\left(\frac{y'}{s'}\right)\right] - \left[\frac{B\kappa}{s'}\left(\frac{y'}{s'}\right)\right]', \tag{103a}$$

$$V = \left[(T_a - B\kappa^2)\frac{y'}{s'} - B\kappa\left(\frac{s''}{s'^2}\right)\left(\frac{x'}{s'}\right)\right] + \left[\frac{B\kappa}{s'}\left(\frac{x'}{s'}\right)\right]', \tag{103b}$$

consequently, one obtains

$$\mathbf{P}' = \left[(T_a - B\kappa^2)\frac{\mathbf{r}_P'}{s'} - B\left(\frac{s''}{s'^3}\right)\frac{\partial}{\partial\alpha}\left(\frac{\mathbf{r}_P'}{s'}\right)\right]' - \left[\frac{B}{s'^2}\frac{\partial}{\partial\alpha}\left(\frac{\mathbf{r}_P'}{s'}\right)\right]''. \tag{104}$$

Note that

$$\frac{\partial}{\partial\alpha}\left(\frac{\mathbf{r}_P'}{s'}\right) = \frac{\partial}{\partial\alpha}\left(\frac{x'}{s'}\right)\hat{\mathbf{i}} + \frac{\partial}{\partial\alpha}\left(\frac{y'}{s'}\right)\hat{\mathbf{j}} = (\kappa y')\hat{\mathbf{i}} + (-\kappa x')\hat{\mathbf{j}} = \hat{\mathbf{t}}' = \theta'\hat{\mathbf{n}}. \tag{105}$$

Utilizing Eqs. (53) and (104), Eq. (101) can be transformed into the displacement-based form:

$$\begin{aligned} & s'(m_P + m_i)\frac{\partial^2\mathbf{r}_P}{\partial t^2} + s'm_i\left(\frac{2V_{FP}}{s'}\right)\frac{\partial^2\mathbf{r}_P}{\partial\alpha\,\partial t} + \left[\frac{B}{s'^2}\frac{\partial}{\partial\alpha}\left(\frac{\mathbf{r}_P'}{s'}\right)\right]'' \\ & - \left[(T_a - B\kappa^2)\frac{\mathbf{r}_P'}{s'} - B\left(\frac{s''}{s'^3}\right)\frac{\partial}{\partial\alpha}\left(\frac{\mathbf{r}_P'}{s'}\right)\right]' + s'm_i\left(\frac{V_{FP}}{s'}\right)^2\frac{\partial^2\mathbf{r}_P}{\partial\alpha^2} \\ & + s'm_i\left[\frac{V_{FP}V_{FP}'}{s'^2} - \frac{V_{FP}\dot{s}'}{s'^2} - \frac{V_{FP}^2 s''}{s'^3}\right]\frac{\partial\mathbf{r}_P}{\partial\alpha} = s'\mathbf{f}_H - s'w_a\hat{\mathbf{j}} - s'm_i\left[\frac{\dot{V}_{FP}}{s'}\right]\frac{\partial\mathbf{r}_P}{\partial\alpha}. \end{aligned} \tag{106}$$

If $\alpha = s$ is used and the internal flow effect is excluded, Eq. (106) is reduced to

$$m_P\ddot{\mathbf{r}}_P + (B\mathbf{r}_P'')'' - [(T_a - B\kappa^2)\mathbf{r}_P']' = \mathbf{f}_H - w_a\hat{\mathbf{j}}, \tag{107}$$

which is compatible with the vector equation of motion of slender rods given by Garrett (1982).

## 4. Vectorial formulation

Based on the vectorial method, the fundamentals of large strain modelling proposed in Section 2 are employed to develop large strain formulations of extensible flexible marine pipes transporting fluid as follows.

*Step* 1: Converting the real system of the pipe column into the apparent systems of the pipe and transported fluid by the apparent tension concept (Section 2.4).

*Step* 2: Using the Newtonian derivation for the apparent systems of the pipe and transported fluid.

*Step* 3: Integrating the individual systems of the pipe and transported fluid into the overall apparent system, which is subjected to the apparent weight (Section 2.4), hydrodynamic forces exerted by external and internal flows (Section 2.5), and inertial forces of the pipe.

*Step* 4: Applying the extensible elastica theory (Section 2.3) on the apparent system to obtain the constitutive equations.

### *4.1. Step 2: Using the Newtonian derivation for the apparent systems*

Consider Fig. 4(q). The apparent system of the transported fluid element with the length $s'\,\mathrm{d}\alpha$ is subjected to (i) the internal pressure $p_i$; (ii) the internal fluid weight $m_i g$; (iii) the inertial forces $m_i a_{Fn}$ and $m_i a_{Ft}$; and (iv) the normal reaction $f_{rn}$ and the wall-shear friction $\tau_w$. Note again that $\alpha$ could be any parameter used to define the elastic curve of the pipe, and $()' = \partial()/\partial\alpha$. Applying Newton's second law in normal and tangential directions, one obtains

$$\sum F_n = 0 : f_{rn}s' = (p_i A_i)\theta' - (m_i g \sin\theta - m_i a_{Fn})s', \tag{108}$$

$$\sum F_t = 0 : \tau_w s' = (p_i A_i)' + (m_i g \cos\theta + m_i a_{Ft})s', \tag{109}$$

in which $(s, \theta)$ are the coordinates of arc length and rotation. Similarly, for the apparent system of the pipe element as shown in Fig. 4(p), applying Newton's second law in normal and tangential directions yields

$$\sum F_n = 0 : f_{rn}s' = -Q' + (T + T_{tri} + p_e A_e)\theta' + [f_{Hn} + (m_P - m_e)g \sin\theta - m_P a_{Pn}]s', \tag{110}$$

$$\sum F_t = 0 : \tau_w s' = Q\theta' + (T + T_{tri} + p_e A_e)' + [f_{Ht} - (m_P - m_e)g \cos\theta - m_P a_{Pt}]s', \tag{111}$$

$$\sum M_o = 0 : M' = Qs', \tag{112}$$

where $T$, $Q$, and $M$ are the true wall tension, shear, and bending moment, respectively, $p_e$ the external pressure, $f_{Hn}$ and $f_{Ht}$ the hydrodynamic forces of external fluid given by Eq. (34), $m_P g$ the pipe weight, $-m_e g$ the buoyancy force, $m_P a_{Pn}$ and $m_P a_{Pt}$ the inertial forces of the pipe, and $T_{tri}$ the tension induced by triaxial pressures given by Eq. (22c).

### *4.2. Step 3: Integrating the individual systems of the pipe and transported fluid into the overall apparent system*

The relationship between Eqs. (108) and (110), and Eqs. (109) and (111), respectively indicates that the interaction between the pipe and the transported fluid is such that physically the reaction $f_{rn}$ and the friction $\tau$ have the effects of:

- transmitting the effect of hydrostatic and hydrodynamic pressures of transported fluid represented by the right-hand side terms in Eqs. (108) and (109) into the pipe wall through the left-hand side terms in Eqs. (110) and (111), and
- conversely, transmitting the effect of resultant forces in pipe wall represented by the right-hand side terms in Eqs. (110) and (111) into transported fluid through the left-hand side terms in Eqs. (108) and (109).

The former effect induces deformation of the pipe, and the latter alters the characteristics of the internal flow of transported fluid as described by Proposition 1.

The interaction links together the individual systems of the pipe and transported fluid into the overall system. Using this fact, one substitutes Eq. (108) into Eq. (110), and Eq. (109) into Eq. (111) to obtain

$$\Sigma F_n = 0 : \quad Q' - T_a\theta' - s'(w_a \sin\theta + f_{Hn} - m_P a_{Pn} - m_i a_{Fn}) = 0, \tag{113}$$

$$\Sigma F_t = 0 : \quad -T_a' - Q\theta' - s'(-w_a \cos\theta + f_{Ht} - m_P a_{Pt} - m_i a_{Ft}) = 0, \tag{114}$$

where $w_a$ and $T_a$ are referred to as the apparent weight and the apparent tension, as given by Eqs. (28) and (29). The governing differential Eqs. (112)–(114) describe the nonlinear behaviour of the overall apparent system of the pipe.

Comparing Eqs. (113) and (114) with Eqs. (99) and (100), we can see that the vectorial method yields the same force-based strong formulation as that obtained from the virtual work method. Thus exact agreement between the virtual work and vectorial formulations is confirmed.

### 4.3. Step 4: Applying the extensible elastica theory on the apparent system

On the apparent system, the axial force appears to be the apparent tension $T_a$ rather than the true wall axial force $N$ of the real system. Applying the extensible elastica theory on the apparent system therefore deals with replacing the axial force $N$ in the constitutive Eqs. (17b), (18b) and (19b) by the apparent tension $T_a$. As a result, Eqs. (64) are obtained as the constitutive equations of the apparent system.

Based on the foregoing derivations along with the geometric relations, the governing equations for the vectorial formulation are summarized as follows:

(a) *Geometric relations*:

$$x'/s' = \sin\theta, \quad y'/s' = \cos\theta, \quad \kappa = \theta'/s' = (x''y' - x'y'')/s'^3. \tag{115a–c}$$

(b) *Constitutive equations*:

$$T_a = E\tilde{A}_P\varepsilon, \quad M = B\kappa. \tag{116a, b}$$

(c) *Equilibrium equations*:

$$M' = s'Q, \tag{117}$$

$$Q' = T_a\theta' + s'[f_{Hn} + w_a\sin\theta - (m_P a_{Pn} + m_i a_{Fn})], \tag{118}$$

$$T_a' = -Q\theta' - s'[f_{Ht} - w_a\cos\theta - (m_P a_{Pt} + m_i a_{Ft})]. \tag{119}$$

## 5. Nonlinear dynamic, large amplitude vibration models

Based on the virtual work and the vectorial formulations, the governing equations describing nonlinear dynamics of the flexible marine pipe have been achieved in the three weak forms such as Eqs. (82)–(85), (86)–(90), and (91)–(96), and in the one strong form such as Eqs. (97)–(100), or Eqs. (101) and (106), or Eqs. (115)–(119). Hence, large amplitude vibration models of the pipe may be generated in four ways, namely from any of the three weak forms or the strong form. However, if the weak forms are employed, the intermediate procedure will require application of some approximate method such as the Rayleigh–Ritz method, the assumed-modes method, or the finite element method. A drawback is that these methods are applicable to self-adjoint systems alone. On the other hand, the models obtained via this approach are concerned with integral equations.

On the other hand, in the case where the strong form is exploited for creating the models, there is no need for any approximate method to be used during the process, and the obtained models deal with differential equations. This yields the possibility of using a broad range of numerical solution methods, including the weighted residuals methods, which are applicable to both self-adjoint and nonself-adjoint systems. For the sake of generality in obtaining the model solution, the strong form thus seems preferable to the weak forms. Derivation of the nonlinear dynamic models based on the strong form given by Eq. (106) is as follows.

### 5.1. Large amplitude vibration models in the Cartesian system

By utilizing Eqs. (54) and introducing the position vector in the Cartesian system

$$\mathbf{x} = \{x \quad y\}^{\mathrm{T}}, \tag{120a}$$

one has the gyroscopic matrix

$$\mathbf{g} = \frac{m_i V_i}{s'^2}\begin{bmatrix} 2s'^2 - x'^2 & -x'y' \\ -x'y' & 2s'^2 - y'^2 \end{bmatrix}, \tag{120b}$$

the bending stiffness matrices

$$\mathbf{k}_{b1} = \frac{B}{s'^5}\begin{bmatrix} y'^2 & -x'y' \\ -x'y' & x'^2 \end{bmatrix}, \quad \mathbf{k}_{b2} = \frac{B\kappa}{s'^4}\begin{bmatrix} 2x'y' & y'^2 - x'^2 \\ y'^2 - x'^2 & -2x'y' \end{bmatrix}, \tag{120c, d}$$

and the axial stiffness matrices

$$\mathbf{k}_{t1} = \frac{(T_a - m_i V_i^2)}{s'^3}\begin{bmatrix} -y'^2 & x'y' \\ x'y' & -x'^2 \end{bmatrix}, \quad \mathbf{k}_{t2} = -\left(\frac{T_a' - m_i V_i V_i'}{s'}\right)\begin{bmatrix} 1 & 0 \\ 0 & 1 \end{bmatrix}, \tag{120e, f}$$

and one can express that

$$s' m_i \left[\left(\frac{V_{FP}}{s'}\right)^2 \frac{\partial^2 \mathbf{r}_P}{\partial \alpha^2} - \left(\frac{V_{FP}^2 s''}{s'^3}\right)\frac{\partial \mathbf{r}_P}{\partial \alpha}\right] = m_i V_i^2 \left(\frac{\mathbf{r}_P'}{s'}\right)', \tag{121a}$$

$$s' m_i \left[\left(\frac{2V_{FP}}{s'}\right)\frac{\partial^2 \mathbf{r}_P}{\partial \alpha\, \partial t} - \left(\frac{V_{FP}\dot{s}'}{s'^2}\right)\frac{\partial \mathbf{r}_P}{\partial \alpha}\right] = \mathbf{g}\dot{\mathbf{x}}' \tag{121b}$$

$$\frac{B}{s'^2}\frac{\partial}{\partial \alpha}\left(\frac{\mathbf{r}_P'}{s'}\right) = \mathbf{k}_{b1}\mathbf{x}'', \tag{121c}$$

$$(T_a - B\kappa^2)\frac{\mathbf{r}_P'}{s'} - B\left(\frac{s''}{s'^3}\right)\frac{\partial}{\partial \alpha}\left(\frac{\mathbf{r}_P'}{s'}\right) = T_a \frac{\mathbf{x}'}{s'} - \mathbf{k}_{b2}\mathbf{x}'', \tag{121d}$$

$$\left(T_a \frac{\mathbf{r}_P'}{s'}\right)' - m_i V_i^2 \left(\frac{\mathbf{r}_P'}{s'}\right)' = -\mathbf{k}_{t1}\mathbf{x}'' - \mathbf{k}_{t2}\mathbf{x}'. \tag{121e}$$

By substituting Eqs. (36) and (121) into Eq. (106) together with some manipulation, the nonlinear dynamic, large amplitude vibration model in the Cartesian system is obtained as

$$\mathbf{m}\ddot{\mathbf{x}} + \mathbf{c}\dot{\mathbf{x}} + \mathbf{g}\dot{\mathbf{x}}' + (\mathbf{k}_{b1}\mathbf{x}'')'' + (\mathbf{k}_{b2}\mathbf{x}'')' + \mathbf{k}_{t1}\mathbf{x}'' + \mathbf{k}_{t2}\mathbf{x}' = \mathbf{f}, \tag{122}$$

where the total mass matrix is

$$\mathbf{m} = s'(m_P + m_i + C_a^*)\begin{bmatrix} 1 & 0 \\ 0 & 1 \end{bmatrix}, \tag{123a}$$

the hydrodynamic damping matrix is

$$\mathbf{c} = s'\begin{bmatrix} C_{eqx}^* & C_{eqxy}^* \\ C_{eqxy}^* & C_{eqy}^* \end{bmatrix}, \tag{123b}$$

and the external load vector is

$$\mathbf{f} = \begin{Bmatrix} f_x \\ f_y \end{Bmatrix} = s'\begin{Bmatrix} C_{Dx}^* V_{Hx}^2 + 2C_{Dxy1}^* V_{Hx}V_{Hy} + C_{Dxy2}^* V_{Hy}^2 + C_M^* \dot{V}_{Hx} - m_i \dot{V}_i x'/s' \\ C_{Dy}^* V_{Hy}^2 + 2C_{Dxy2}^* V_{Hx}V_{Hy} + C_{Dxy1}^* V_{Hx}^2 + C_M^* \dot{V}_{Hy} - w_a - m_i \dot{V}_i y'/s' \end{Bmatrix}. \tag{123c}$$

In Eq. (122), the effect of large axial strain and the Poisson's ratio effect contribute in all the coefficient matrices, especially to the terms of the combined tension $T_a - m_i V_i^2$ and the tension gradient $T_a' - m_i V_i V_i'$ in the axial stiffness matrices. It is also evident that the effect of transported fluid is

- to add the inertial force of transported mass into the total mass matrix,
- to provide the negative damping force in the gyroscopic matrix,
- to reduce the internal tension and axial stiffness of the system in the axial stiffness matrices,
- to provide an excitation term in the external load vector.

### 5.2. Large amplitude vibration models in the natural system

Introducing the bending coefficients in the natural system

$$b_{1n} = \frac{B}{s'^3}, \quad b_{2n} = \frac{2B'}{s'^3} - \frac{3B}{s'^3}\left(\frac{s''}{s'}\right), \quad b_{3n} = \frac{B'}{s'^3} - \frac{B}{s'^3}\left(\frac{s''}{s'}\right), \tag{124a−c}$$

$$b_{4n} = \frac{B''}{s'^3} - \frac{3B'}{s'^3}\left(\frac{s''}{s'}\right) - \frac{B}{s'^3}\left(\frac{s'''}{s'}\right) + \frac{3B}{s'^3}\left(\frac{s''}{s'}\right)^2, \tag{124d}$$

one can express that

$$Q = \frac{(B\kappa)'}{s'} = \frac{1}{s'}\frac{\partial}{\partial\alpha}\left(B\frac{\theta'}{s'}\right) = b_{1n}(s'\theta'') + b_{3n}(s'\theta'), \tag{125}$$

$$Q' = \left[\frac{(B\kappa)'}{s'}\right]' = b_{1n}(s'\theta''') + b_{2n}(s'\theta'') + b_{4n}(s'\theta'), \tag{126}$$

where the expressions for $s'$ and $\theta$ can be determined from the geometric relations

$$s'\sin(\theta - \theta_o) = u_n' + v_n\theta_o', \quad s'\cos(\theta - \theta_o) = s_o' + v_n' - u_n\theta_o', \tag{127a, b}$$

$$s'^2 = (u_n' + v_n\theta_o')^2 + (s_o' + v_n' - u_n\theta_o')^2, \quad \tan(\theta - \theta_o) = \frac{u_n' + v_n\theta_o'}{s_o' + v_n' - u_n\theta_o'}. \tag{127c, d}$$

By substituting Eqs. (34), (58a), (60), (125), and (126) into Eq. (101) together with some manipulation, the large amplitude vibration model in the natural system is obtained as

$$\mathbf{m}\begin{Bmatrix} \ddot{u}_n \\ \ddot{v}_n \end{Bmatrix} + \mathbf{c}_n\begin{Bmatrix} \dot{u}_n \\ \dot{v}_n \end{Bmatrix} + \mathbf{g}_n\begin{Bmatrix} s'\dot{\theta} \\ \dot{s}' \end{Bmatrix} + \mathbf{k}_{b1n}\begin{Bmatrix} s'\theta''' \\ s'\theta'\theta'' \end{Bmatrix} + \mathbf{k}_{b2n}\begin{Bmatrix} s'\theta'' \\ s'\theta'^2 \end{Bmatrix} + \mathbf{k}_{t1n}\begin{Bmatrix} s'\theta' \\ 0 \end{Bmatrix} + \mathbf{k}_{t2n}\begin{Bmatrix} 0 \\ s' \end{Bmatrix} = \mathbf{f}_n, \tag{128}$$

where the hydrodynamic damping matrix is

$$\mathbf{c}_n = s'\begin{bmatrix} C^*_{eqn} & 0 \\ 0 & C^*_{eqt} \end{bmatrix}, \tag{129a}$$

the gyroscopic matrix is

$$\mathbf{g}_n = m_i V_i \begin{bmatrix} 2 & 0 \\ 0 & 1 \end{bmatrix}, \tag{129b}$$

the bending stiffness matrices are

$$\mathbf{k}_{b1n} = \begin{bmatrix} b_{1n} & 0 \\ 0 & -b_{1n} \end{bmatrix}, \quad \mathbf{k}_{b2n} = \begin{bmatrix} b_{2n} & 0 \\ 0 & -b_{3n} \end{bmatrix}, \tag{129c, d}$$

the axial stiffness matrices are

$$\mathbf{k}_{t1n} = \left[b_{4n} - \frac{(T_a - m_i V_i^2)}{s'}\right]\begin{bmatrix} 1 & 0 \\ 0 & 0 \end{bmatrix}, \quad \mathbf{k}_{t2n} = -\left(\frac{T_a' - m_i V_i V_i'}{s'}\right)\begin{bmatrix} 0 & 0 \\ 0 & 1 \end{bmatrix}, \tag{129e, f}$$

and the external load vector is

$$\mathbf{f}_n = \begin{Bmatrix} f_n \\ f_t \end{Bmatrix} = s'\begin{Bmatrix} C^*_{Dn}V^2_{Hn} + C^*_M\dot{V}_{Hn} + w_a\sin\theta \\ C^*_{Dt}V^2_{Ht} + C^*_M\dot{V}_{Ht} - w_a\cos\theta - m_i\dot{V}_i \end{Bmatrix}. \tag{129g}$$

It is evident that in the natural coordinate system there is no coupling term in all the coefficient matrices. Note that for the lower order analysis, the following approximations by two-term binomial expansion may be used in Eq. (128):

$$s' \approx s_o' + v_n' - u_n\theta_o', \quad \theta \approx \theta_o + (u_n' + v_n\theta_o')/s', \tag{130a, b}$$

$$\dot{s}' \approx \dot{v}_n' - \dot{u}_n\theta_o', \quad s'\dot{\theta} \approx \dot{u}_n' + \dot{v}_n\theta_o', \quad s'\theta' \approx s_o'\theta_o' + u_n'' + 2v_n'\theta_o', \tag{130c−e}$$

$$s'\theta'' \approx s'_o\theta''_o + u'''_n + v''_n\theta'_o, \quad s'\theta''' \approx s'_o\theta'''_o + u''''_n + v'''_n\theta'_o, \tag{130f, g}$$

$$s'\theta'^2 \approx s'_o\theta'^2_o + 2u''_n\theta'_o, \quad s'\theta'\theta'' \approx s'_o\theta'_o\theta''_o + u'''_n\theta'_o. \tag{130h, i}$$

### 5.3. First-order models for large amplitude vibrations

Once Eqs. (36) and (56) are substituted into Eqs. (97) and (98), the second-order model of large amplitude vibrations of the pipe is established. To reduce the second-order system to the first-order system, the velocity expressions following Eqs. (131a)–(131c) are introduced. By adopting Eqs. (115)–(117) and (123c), the first-order model can be obtained as

$$\frac{\partial x}{\partial t} = V_{Px}, \tag{131a}$$

$$\frac{\partial y}{\partial t} = V_{Py}, \tag{131b}$$

$$\frac{\partial \theta}{\partial t} = V_{P\theta}, \tag{131c}$$

$$\frac{\partial x}{\partial \alpha} = s' \sin\theta, \tag{132a}$$

$$\frac{\partial y}{\partial \alpha} = s' \cos\theta, \tag{132b}$$

$$\frac{\partial \theta}{\partial \alpha} = s' \frac{M}{B}, \tag{132c}$$

$$\frac{\partial M}{\partial \alpha} = s'(V\sin\theta - H\cos\theta), \tag{132d}$$

$$\begin{aligned}\frac{\partial H}{\partial \alpha} = {} & s'(m_P + m_i + C_a^*)\frac{\partial V_{Px}}{\partial t} + m_i V_i(2 - \sin^2\theta)\frac{\partial V_{Px}}{\partial \alpha} - m_i V_i \sin\theta\cos\theta\frac{\partial V_{Py}}{\partial \alpha} \\ & + s'\left(C^*_{eqx}V_{Px} + C^*_{eqxy}V_{Py} + m_i V_i^2\frac{M}{B}\cos\theta + \frac{m_i V_i V_i'}{s'}\sin\theta\right) - f_x,\end{aligned} \tag{132e}$$

$$\begin{aligned}\frac{\partial V}{\partial \alpha} = {} & s'(m_P + m_i + C_a^*)\frac{\partial V_{Py}}{\partial t} - m_i V_i \sin\theta\cos\theta\frac{\partial V_{Px}}{\partial \alpha} + m_i V_i(2 - \cos^2\theta)\frac{\partial V_{Py}}{\partial \alpha} \\ & + s'\left(C^*_{eqxy}V_{Px} + C^*_{eqy}V_{Py} - m_i V_i^2\frac{M}{B}\sin\theta + \frac{m_i V_i V_i'}{s'}\cos\theta\right) - f_y.\end{aligned} \tag{132f}$$

If $\alpha = s$ is used, and hydrodynamic effects due to external flow, and unsteady, nonuniform internal flow are excluded, Eqs. (132) become

$$\frac{\partial x}{\partial s} = \sin\theta, \tag{133a}$$

$$\frac{\partial y}{\partial s} = \cos\theta, \tag{133b}$$

$$\frac{\partial \theta}{\partial s} = \frac{M}{B}, \tag{133c}$$

$$\frac{\partial M}{\partial s} = V\sin\theta - H\cos\theta, \tag{133d}$$

$$\frac{\partial H}{\partial s} = (m_P + m_i)\frac{\partial V_{Px}}{\partial t} + 2m_i V_i V_{P\theta}\cos\theta + m_i V_i^2\frac{M}{B}\cos\theta, \tag{133e}$$

$$\frac{\partial V}{\partial s} = (m_P + m_i)\frac{\partial V_{Py}}{\partial t} - 2m_i V_i V_{P\theta}\sin\theta - m_i V_i^2\frac{M}{B}\sin\theta + (m_P + m_i)g. \tag{133f}$$

Note that

$$\frac{\partial V_{Px}}{\partial t} = \frac{\partial^2 x}{\partial t^2}, \quad V_{P\theta}\cos\theta = \frac{\partial V_{Px}}{\partial s} = \frac{\partial^2 x}{\partial s\,\partial t}, \quad -V_{P\theta}\sin\theta = \frac{\partial V_{Py}}{\partial s} = \frac{\partial^2 y}{\partial s\,\partial t}, \tag{134a, b}$$

and

$$\frac{\partial V_{Py}}{\partial t} = \frac{\partial^2 y}{\partial t^2}, \quad \frac{M}{B}\cos\theta = \frac{\partial\theta}{\partial s}\frac{\partial y}{\partial s} = \frac{\partial^2 x}{\partial s^2}, \quad -\frac{M}{B}\sin\theta = -\frac{\partial\theta}{\partial s}\frac{\partial x}{\partial s} = \frac{\partial^2 y}{\partial s^2}. \tag{134c, d}$$

Eqs. (133) describe the nonlinear dynamics of an onshore pipe steadily conveying fluid (Atanackovic, 1997; Païdoussis, 1998).

## 6. Nonlinear static equilibrium models

The static equilibrium models are derived by eliminating the time-dependent terms in the nonlinear dynamic equations. As a result, all parameters at the displaced state contained in the nonlinear dynamic equations will alter to the parameters at the equilibrium state for nonlinear static equilibrium models.

### 6.1. Nonlinear static models in the Cartesian system

Eliminating the time-dependent terms in Eq. (122), and replacing the variables at the displaced state by those at the equilibrium state, one obtains the static equilibrium model as

$$(\mathbf{k}_{b1o}\mathbf{x}''_o)'' + (\mathbf{k}_{b2o}\mathbf{x}''_o)' + \mathbf{k}_{t1o}\mathbf{x}''_o + \mathbf{k}_{t2o}\mathbf{x}'_o = \mathbf{f}_o, \tag{135}$$

where the position vector is

$$\mathbf{x}_o = \{x_0 \quad y_0\}^{\mathrm{T}}, \tag{136a}$$

the bending stiffness matrices are

$$\mathbf{k}_{b1o} = \frac{B_o}{s_o'^5}\begin{bmatrix} y_o'^2 & -x'_o y'_o \\ -x'_o y'_o & x_o'^2 \end{bmatrix}, \quad \mathbf{k}_{b2} = \frac{B_o\kappa_o}{s_o'^4}\begin{bmatrix} 2x'_o y'_o & y_o'^2 - x_o'^2 \\ y_o'^2 - x_o'^2 & -2x'_o y'_o \end{bmatrix}, \tag{136b, c}$$

and the axial stiffness matrices are

$$\mathbf{k}_{t1o} = \frac{(T_{ao} - m_{io}V_{io}^2)}{s_o'^3}\begin{bmatrix} -y'_o 2 & x'_o y'_o \\ x'_o y'_o & -x_o'^2 \end{bmatrix}, \quad \mathbf{k}_{t2o} = -\left(\frac{T'_{ao} - m_{io}V_{io}V'_{io}}{s'_o}\right)\begin{bmatrix} 1 & 0 \\ 0 & 1 \end{bmatrix}, \tag{136d, e}$$

and the external load vector is

$$\mathbf{f}_o = \begin{Bmatrix} f_{xo} \\ f_{yo} \end{Bmatrix} = s'_o\begin{Bmatrix} C^*_{Dxo}V^2_{Hxo} + 2C^*_{Dxy1o}V_{Hxo}V_{Hyo} + C^*_{Dxy2o}V^2_{Hyo} \\ C^*_{Dyo}V^2_{Hyo} + 2C^*_{Dxy2o}V_{Hxo}V_{Hyo} + C^*_{Dxy1o}V^2_{Hxo} - w_{ao} \end{Bmatrix}. \tag{136f}$$

### 6.2. Nonlinear static models in the natural system

Similarly, eliminating the time-dependent terms in Eq. (128) yields the static model

$$\mathbf{k}_{b1no}\begin{Bmatrix} s'_o\theta'''_o \\ s'_o\theta'_o\theta''_o \end{Bmatrix} + \mathbf{k}_{b2no}\begin{Bmatrix} s'_o\theta''_o \\ s'_o\theta_o'^2 \end{Bmatrix} + \mathbf{k}_{t1no}\begin{Bmatrix} s'_o\theta'_o \\ 0 \end{Bmatrix} + \mathbf{k}_{t2no}\begin{Bmatrix} 0 \\ s'_o \end{Bmatrix} = \mathbf{f}_{no}, \tag{137}$$

where the bending stiffness matrices are

$$\mathbf{k}_{b1no} = \begin{bmatrix} b_{1no} & 0 \\ 0 & -b_{1no} \end{bmatrix}, \quad \mathbf{k}_{b2no} = \begin{bmatrix} b_{2no} & 0 \\ 0 & -b_{3no} \end{bmatrix}, \tag{138a, b}$$

in which the bending coefficients are

$$b_{1no} = \frac{B_o}{s_o'^3}, \quad b_{2no} = \frac{2B'_o}{s_o'^3} - \frac{3B_o}{s_o'^3}\left(\frac{s''_o}{s'_o}\right), \quad b_{3no} = \frac{B'_o}{s_o'^3} - \frac{B_o}{s_o'^3}\left(\frac{s''_o}{s'_o}\right), \tag{139c–e}$$

$$b_{4no} = \frac{B''_o}{s'^3_o} - \frac{3B'_o}{s'^3_o}\left(\frac{s''_o}{s'_o}\right) - \frac{B_o}{s'^3_o}\left(\frac{s'''_o}{s'_o}\right) + \frac{3B_o}{s'^3_o}\left(\frac{s''_o}{s'_o}\right)^2, \tag{139f}$$

the axial stiffness matrices are

$$\mathbf{k}_{t1no} = \left[b_{4no} - \frac{(T_{ao} - m_{io}V_{io}^2)}{s'_o}\right]\begin{bmatrix}1 & 0\\ 0 & 0\end{bmatrix}, \quad \mathbf{k}_{t2no} = -\left(\frac{T'_{ao} - m_{io}V_{io}V'_{io}}{s'_o}\right)\begin{bmatrix}0 & 0\\ 0 & 1\end{bmatrix}, \tag{139g, h}$$

and the external load vector is

$$\mathbf{f}_{no} = \begin{Bmatrix} f_{no} \\ f_{to} \end{Bmatrix} = s'_o \begin{Bmatrix} C^*_{Dno}V^2_{Hno} + w_{ao}\sin\theta_o \\ C^*_{Dto}V^2_{Hto} - w_{ao}\cos\theta_o \end{Bmatrix}. \tag{139i}$$

### 6.3. First-order models for nonlinear static equilibriums

Likewise, once the time-dependent terms in Eqs. (131) and (132) are eliminated, the system of the first-order differential equilibrium equations is obtained as

$$\frac{dx_o}{d\alpha} = s'_o \sin\theta_o, \tag{140a}$$

$$\frac{dy_o}{d\alpha} = s'_o \cos\theta_o, \tag{140b}$$

$$\frac{d\theta_o}{d\alpha} = s'_o\frac{M_o}{B_o}, \tag{140c}$$

$$\frac{dM_o}{d\alpha} = s'_o(V_o\sin\theta_o - H_o\cos\theta_o) = s'_oQ_o, \tag{140d}$$

$$\frac{dH_o}{d\alpha} = s'_o\left(m_{io}V_{io}^2\frac{M_o}{B_o}\cos\theta_o + \frac{m_{io}V_{io}V'_{io}}{s'_o}\sin\theta_o\right) - f_{xo}, \tag{140e}$$

$$\frac{\partial V_o}{\partial\alpha} = s'_o\left(-m_{io}V_{io}^2\frac{M_o}{B_o}\sin\theta_o + \frac{m_{io}V_{io}V'_{io}}{s'_o}\cos\theta_o\right) - f_{yo}, \tag{140f}$$

$$\frac{dQ_o}{d\alpha} = (T_{ao} - m_{io}V_{io}^2)\frac{d\theta_o}{d\alpha} + f_{no}, \tag{140g}$$

$$\frac{dT_{ao}}{d\alpha} = -Q_o\frac{d\theta_o}{d\alpha} + m_{io}V_{io}\frac{dV_{io}}{d\alpha} - f_{to}. \tag{140h}$$

The boundary-value problem of the system of the first-order ordinary differential equations (140) can be solved directly by numerical integrations. Application of the system of equations (140) to a nonlinear bucking analysis of extensible flexible marine pipes transporting fluid via the method of adjacent nonlinear equilibrium has been demonstrated by Chucheepsakul and Monprapussorn (2001).

## 7. Choices of the independent variable

One salient feature of the large strain formulations presented in this work is that the independent variable $\alpha$ used in the formulations provides flexibility in the choice of parameters defining elastic curves. The formulations therefore allow users to select the independent variable that is most efficient for their own problem solution. For example, analysis of flexible marine pipes as shown in Fig. 1 has at least three alternatives for the independent variable $\alpha$ such as the vertical coordinate $y$, the offset distance $x$, and the arc length $s$.

The advantage of using $\alpha = y$ is that the total water depth or the boundary condition is known initially, while by using $\alpha = x$ the boundary condition is known if the offset at the top end of the pipe can be assumed to be static, and is unknown if the offset is dynamic. If one uses $\alpha = s$, the boundary condition is always unknown, because the total arc length changes after deformation. The problem for which the boundary condition is unknown becomes much more difficult, and requires specific treatment.

However, the disadvantage of using $\alpha = y$ is that if elastic curves after large displacements form like the U-shape or the semi-U-shape as shown in Figs. 1(b) and (c), the vertical position is no longer a one-to-one function for all points on the elastic curves. Consequently, $\alpha = y$ is not an effective choice in this case. Likewise, using $\alpha = x$ encounters the same difficulty when the elastic curves after large displacements develop akin to the C-shape or the semi-C-shape. In these troublesome cases, using $\alpha = s$ becomes the best way, because arc length is an intrinsic property, and thus is always a one-to-one function for all points of the elastic curves.

Therefore for flexible marine pipes which do not face the problem of elastic curves having a U-shape, such as the high-tensioned pipes as shown in Fig. 1(a), using $\alpha = y$ is sufficient. However, if the pipes confront the problem that occurs in the case of low-tensioned pipes as shown in Figs. 1(b) and (c), $\alpha = s$ should be employed. It should be noted that in addition to the three alternatives of $\alpha$ as exemplified earlier, there are still other choices of $\alpha$ such as the span length, the rotational angle, and so on, which may be employed if efficient.

## 8. Extension to other applications

The present formulations are applicable to large strain analysis not only of flexible marine pipes, but also of any kind of elastica structures listed below.

(a) *Onshore pipes*: The effect of external fluid would be excluded from the present models.
(b) *Submerged pipes*: The hydrodynamic pressure effect of external fluid would be excluded.
(c) *Marine cables*: Bending rigidity and influence of internal fluid would be excluded.
(d) *Submerged cables*: Bending rigidity, influence of internal fluid, and hydrodynamic pressure effect of external fluid would be excluded from the present models.
(e) *Onshore cables and strings*: Bending rigidity, and influences of internal and external fluids would be excluded from the present models.
(f) *Elastic rods*, *long columns*, *and long beams*: Influences of external and internal fluids would be excluded from the present models.

Even though the present models are intended for elastica structures with environment-induced initial curvatures, the models can still be extended to elastica structures with man-made initial curvatures such as curved beams and arches by considering $\bar{\kappa} \neq 0$ in application of the extensible elastica theory presented in this paper.

## 9. Conclusions

A literature review has shown that the effects of axial deformation, internal flow, and Poisson's ratio effect can be significant in the behaviour of flexible marine pipes. To take account of the combined action of these effects in flexible marine pipe analysis, large strain formulations are needed. The essential mathematical principles for large strain modelling are developed in this paper. These include original developments of the apparent tension concept, and the extensible elastica theories from the viewpoints of total Lagrangian, updated Lagrangian, and Eulerian mechanics. Based on large strain elasticity and the apparent tension concept, it is shown that the Poisson's ratio effect influences the characteristics of internal flow, and induces the apparent tension rather than the effective tension. Therefore, the apparent tension should be used in large strain analysis for general Poisson's ratios.

Based on the proposed mathematical principles, the large strain formulations are developed by the virtual work method and the vectorial method in both Cartesian and natural coordinates. The virtual work method produces large strain models in the three weak forms of integral equations, and one strong form of differential equations, while the vectorial method yields the identical strong form. All the four forms of the models can be used for large strain analysis of the pipe, however, with different aspects of model solutions as summarized in Table 1. Relying upon the strong form, one can create large strain models of large amplitude vibrations and nonlinear static equilibrium of pipes. The advantages of the present models relate to the flexibility offered in choice of the independent variable, and the possibility of applying them to numerous elastica problems, including even some biomechanics applications such as veins conveying fluids inside the human body, and vessels rising water in the xylem of a plant.

Table 1
Alternatives of large strain modeling of flexible marine pipes

| Large strain models by | Governing equations | | Constraint of natural BCs | Solution methods |
|---|---|---|---|---|
| | Equations | Type | | |
| Weak form 1 | (82)–(85) | | None | |
| Weak form 2 | (86), (87), (89), (90) | Integral equations | Some | Limited to assumed mode methods |
| Weak form 3 | (91), (92), (94), (95) | | All | |
| Strong form | (97)–(100), or (101), (106), or (115)–(119) | Differential equations | All | Unlimited |

## Acknowledgements

The authors gratefully acknowledge the support of the Thailand Research Fund (TRF) under Contract No. RTA/03/2543.

## Appendix A. Derivation of extensible elastica theory

Consider Fig. 2(b). Displacements and deformations of the pipe element from the undeformed state (state 1) to the equilibrium state (state 2), and then to the displaced state (state 3) result in changes of

- axial strain at the neutral axis $\bar{\varepsilon} \to \varepsilon_o \to \varepsilon$,
- bending moment $\bar{M} \to M_o \to M$,
- radius of curvature $\bar{r} \to r_o \to r$,
- differential arc length $\mathrm{d}\bar{s} \to \mathrm{d}s_o \to \mathrm{d}s$,
- differential rotation angle $\mathrm{d}\bar{\theta} \to \mathrm{d}\theta_o \to \mathrm{d}\theta$.

Rotations of cross-section from state 1 to 2, from state 2 to 3, and from state 1 to 3 are denoted by $\mathrm{d}\varphi_o = \mathrm{d}\theta_o - \mathrm{d}\bar{\theta}$, $\mathrm{d}\varphi_d = \mathrm{d}\theta - \mathrm{d}\theta_o$, and $\mathrm{d}\varphi = \mathrm{d}\theta - \mathrm{d}\bar{\theta}$, respectively.

In order to describe these changes, the three deformation descriptors previously defined in Section 2.1 are employed. Consequently, the extensible elastica theory can be developed by the total Lagrangian, the updated Lagrangian, and the Eulerian formulations as follows.

### A.1. Total Lagrangian formulation

The total Lagrangian formulation considers total changes from state 1 to 3 by neglecting the intermediate state 2. All changes are measured relative to the original state 1. The theoretical development starts by expressing the undeformed and deformed arc lengths of the fibre at any radius $\varsigma$ as

$$\mathrm{d}\bar{s}_\varsigma = (\bar{r} + \varsigma)\,\mathrm{d}\bar{\theta}, \tag{A.1a}$$

$$\mathrm{d}s_\varsigma = (r + \varsigma)(\mathrm{d}\varphi + \mathrm{d}\bar{\theta}) = r\,\mathrm{d}\theta + \varsigma(\mathrm{d}\varphi + \mathrm{d}\bar{\theta}). \tag{A.1b}$$

Since $\mathrm{d}\bar{\theta} = \mathrm{d}\bar{s}/\bar{r}$ and $\mathrm{d}\theta = \mathrm{d}s/r = (1+\varepsilon)\,\mathrm{d}\bar{s}/r$, Eqs. (A.1) may be written in the form

$$\mathrm{d}\bar{s}_\varsigma = \left(1 + \frac{\varsigma}{\bar{r}}\right)\mathrm{d}\bar{s} = (1 + \varsigma\bar{\kappa})\,\mathrm{d}\bar{s}, \tag{A.2a}$$

$$\mathrm{d}s_\varsigma = (1+\varepsilon)\,\mathrm{d}\bar{s} + \varsigma\left(\mathrm{d}\varphi + \frac{\mathrm{d}\bar{s}}{\bar{r}}\right) = \left(1 + \varepsilon + \varsigma\frac{\mathrm{d}\varphi}{\mathrm{d}\bar{s}} + \varsigma\bar{\kappa}\right)\mathrm{d}\bar{s}, \tag{A.2b}$$

where $\bar{\kappa} = 1/\bar{r}$ and $\kappa = 1/r$ are the curvatures at the undeformed and the displaced states, and

$$\frac{\mathrm{d}\varphi}{\mathrm{d}\bar{s}} = \frac{\mathrm{d}\theta}{\mathrm{d}s}\frac{\mathrm{d}s}{\mathrm{d}\bar{s}} - \frac{\mathrm{d}\bar{\theta}}{\mathrm{d}\bar{s}} = \kappa(1+\varepsilon) - \bar{\kappa}. \tag{A.3}$$

From Definition 4, the TL-strain of the fibre at any radius $\varsigma$ is defined by

$$\varepsilon_\varsigma = \frac{\mathrm{d}s_\varsigma - \mathrm{d}\bar{s}_\varsigma}{\mathrm{d}\bar{s}_\varsigma} = \frac{(\varepsilon + \varsigma(\mathrm{d}\varphi/\mathrm{d}\bar{s}))\,\mathrm{d}\bar{s}}{(1+\varsigma\bar{\kappa})\,\mathrm{d}\bar{s}} = \frac{\varepsilon + \varsigma[\kappa(1+\varepsilon) - \bar{\kappa}]}{1+\varsigma\bar{\kappa}}. \tag{A.4}$$

The stress corresponding to the TL-strain $\sigma_\varsigma = E\varepsilon_\varsigma$ is referred to as the Kirchhoff stress. The axial force and the bending moment due to the Kirchhoff stress can be expressed as

$$N = \int_{\bar{A}_P} \sigma_\varsigma\,\mathrm{d}\bar{A}_P = E\int_{\bar{A}_P}\left[\frac{\varepsilon + \varsigma[\kappa(1+\varepsilon) - \bar{\kappa}]}{1+\varsigma\bar{\kappa}}\right]\mathrm{d}\bar{A}_P, \tag{A.5a}$$

$$M = \int_{\bar{A}_P} \sigma_\varsigma\varsigma\,\mathrm{d}\bar{A}_P = E\int_{\bar{A}_P}\left[\frac{\varepsilon\varsigma + \varsigma^2[\kappa(1+\varepsilon) - \bar{\kappa}]}{1+\varsigma\bar{\kappa}}\right]\mathrm{d}\bar{A}_P, \tag{A.5b}$$

in which $E$ is the elastic modulus and $\bar{A}_P$ is the undeformed cross-sectional area of a pipe.

If the following geometrical properties of the cross-section

$$\bar{A}_P^* = \int_{\bar{A}_P}\frac{\mathrm{d}\bar{A}_P}{1+\varsigma\bar{\kappa}}, \quad \bar{Q}_P^* = \int_{\bar{A}_P}\frac{\varsigma\,\mathrm{d}\bar{A}_P}{1+\varsigma\bar{\kappa}}, \quad \bar{I}_P^* = \int_{\bar{A}_P}\frac{\varsigma^2\,\mathrm{d}\bar{A}_P}{1+\varsigma\bar{\kappa}}. \tag{A.6a–c}$$

are defined, Eqs. (A.5) may be rewritten in the form

$$N = E\bar{A}_P^*\varepsilon + E\bar{Q}_P^*[\kappa(1+\varepsilon) - \bar{\kappa}], \quad M = E\bar{Q}_P^*\varepsilon + E\bar{I}_P^*[\kappa(1+\varepsilon) - \bar{\kappa}]. \tag{A.7a, b}$$

The TL-strain energy due to the TL-strain $\varepsilon_\varsigma$ is measured with respect to the undeformed volume of the pipe $\bar{\forall}_P$. Therefore, its expression is given by

$$U = \int_{\bar{\forall}_P}\frac{\sigma_\varsigma\varepsilon_\varsigma}{2}\,\mathrm{d}\bar{\forall}_P = \int_{\bar{\forall}_P}\frac{\varepsilon_\varsigma^2}{2}\,\mathrm{d}\bar{\forall}_P. \tag{A.8}$$

Taking the first variation of Eq. (A.8), one obtains

$$\delta U = \int_{\bar{\forall}_P} E\varepsilon_\varsigma\delta\varepsilon_\varsigma\,\mathrm{d}\bar{\forall}_P = \int_{\bar{s}}\int_{\bar{A}_P}\sigma_\varsigma\left[\frac{\delta\varepsilon + \varsigma\delta[\kappa(1+\varepsilon) - \bar{\kappa}]}{1+\varsigma\bar{\kappa}}\right]\mathrm{d}\bar{A}_P\,\mathrm{d}\bar{s}. \tag{A.9}$$

For elastica problems, $\varsigma\bar{\kappa} = \varsigma/\bar{r} \ll 1$, thus $1/(1+\varsigma\bar{\kappa}) \approx 1$. Consequently, Eqs. (A.6) yield $\bar{A}_P^* \approx \bar{A}_P$, $\bar{Q}_P^* \approx 0$, and $\bar{I}_P^* \approx \bar{I}_P$. Substituting these conditions in Eqs. (A.4), (A.7), and (A.9), the constitutive equations of the extensible elastica theory can be obtained as

TL-axial strain:

$$\varepsilon_\varsigma = \varepsilon + \varsigma[\kappa(1+\varepsilon) - \bar{\kappa}], \tag{A.10}$$

TL-axial force:

$$N = E\bar{A}_P\varepsilon, \tag{A.11}$$

TL-bending moment:

$$M = E\bar{I}_P[\kappa(1+\varepsilon) - \bar{\kappa}], \tag{A.12}$$

TL-strain energy:

$$\delta U = \int_{\bar{s}}\{N\delta\varepsilon + M\delta[\kappa(1+\varepsilon) - \bar{\kappa}]\}\,\mathrm{d}\bar{s} = \int_{\alpha}[N\delta s' + M\delta(\theta' - \bar{\theta}')]\,\mathrm{d}\alpha \tag{A.13}$$

Note that

$$\delta\varepsilon = \delta\left(\frac{\mathrm{d}s - \mathrm{d}\bar{s}}{\mathrm{d}\bar{s}}\right) = \delta s'/\bar{s}', \quad \delta[\kappa(1+\varepsilon) - \bar{\kappa}] = \delta\left(\frac{\mathrm{d}\theta}{\mathrm{d}\bar{s}} - \frac{\mathrm{d}\bar{\theta}}{\mathrm{d}\bar{s}}\right) = \delta(\theta' - \bar{\theta}')/\bar{s}'.$$

### *A.2. Updated Lagrangian formulation*

The updated Lagrangian formulation considers the two-step changes from state 1 to 2, and then from state 2 to 3. All changes are measured relative to the intermediate state 2. The development starts by expressing the three state arc lengths of the fibre at any $\varsigma$ as

$$\mathrm{d}\bar{s}_\varsigma = (\bar{r} + \varsigma)\,\mathrm{d}\bar{\theta} = \bar{r}\,\mathrm{d}\bar{\theta} + \varsigma(\mathrm{d}\theta_o - \mathrm{d}\varphi_o), \tag{A.14a}$$

$$\mathrm{d}s_o = (r_o + \varsigma)\,\mathrm{d}\theta_o, \tag{A.14b}$$

$$\mathrm{d}s_\varsigma = (r + \varsigma)(\mathrm{d}\varphi_d + \mathrm{d}\theta_o) = \mathrm{r}\,\mathrm{d}\theta + \varsigma(\mathrm{d}\varphi_d + \mathrm{d}\theta_o). \tag{A.14c}$$

Since $\mathrm{d}\bar{\theta} = \mathrm{d}\bar{s}/\bar{r} = (1 - \varepsilon_o)\,\mathrm{d}s_o/\bar{r}$, $\mathrm{d}\theta_o = \mathrm{d}s_o/r_o$, and $\mathrm{d}\theta = \mathrm{d}s/r = (1 + \varepsilon_d)\,\mathrm{d}s_o/r$, Eqs. (A.14) may be written in the form

$$\mathrm{d}\bar{s}_\varsigma = (1 - \varepsilon_o)\,\mathrm{d}s_o + \varsigma\left(\frac{\mathrm{d}s_o}{r_o} - \mathrm{d}\varphi_o\right) = \left(1 - \varepsilon_o + \varsigma\kappa_o - \varsigma\frac{\mathrm{d}\varphi_o}{\mathrm{d}s_o}\right)\mathrm{d}s_o, \tag{A.15a}$$

$$\mathrm{d}s_{o\varsigma} = \left(1 + \frac{\varsigma}{r_o}\right)\mathrm{d}s_o = (1 + \varsigma\kappa_o)\,\mathrm{d}s_o, \tag{A.15b}$$

$$\mathrm{d}s_\varsigma = (1 + \varepsilon_d)\,\mathrm{d}s_o + \varsigma\left(\mathrm{d}\varphi_d + \frac{\mathrm{d}s_o}{r_o}\right) = \left(1 + \varepsilon_d + \varsigma\frac{\mathrm{d}\varphi_d}{\mathrm{d}s_o} + \varsigma\kappa_o\right)\mathrm{d}s_o, \tag{A.15c}$$

where $\bar{\kappa} = 1/\bar{r}$, $\kappa_o = 1/r_o$, and $\kappa = 1/r$ are the curvatures at the three states, and

$$\frac{\mathrm{d}\varphi_o}{\mathrm{d}s_o} = \frac{\mathrm{d}\theta_o}{\mathrm{d}s_o} - \frac{\mathrm{d}\bar{\theta}}{\mathrm{d}\bar{s}}\frac{\mathrm{d}\bar{s}}{\mathrm{d}s_o} = \kappa_o - \bar{\kappa}(1 - \varepsilon_o), \tag{A.16a}$$

$$\frac{\mathrm{d}\varphi_d}{\mathrm{d}s_o} = \frac{\mathrm{d}\theta}{\mathrm{d}s}\frac{\mathrm{d}s}{\mathrm{d}s_o} - \frac{\mathrm{d}\theta_o}{\mathrm{d}s_o} = \kappa(1 + \varepsilon_d) - \kappa_o, \tag{A.16b}$$

$$\frac{\mathrm{d}\varphi}{\mathrm{d}s_o} = \frac{\mathrm{d}\varphi_o}{\mathrm{d}s_o} + \frac{\mathrm{d}\varphi_d}{\mathrm{d}s_o} = \kappa(1 + \varepsilon_d) - \bar{\kappa}(1 - \varepsilon_o). \tag{A.16c}$$

From Definition 4, the UL-strain of the fibre at any radius $\varsigma$ is defined by

$$\varepsilon_\varsigma = \frac{\mathrm{d}s_\varsigma - \mathrm{d}\bar{s}_\varsigma}{\mathrm{d}s_{o\varsigma}} = \frac{\left[\varepsilon_d + \varepsilon_o + \varsigma(\mathrm{d}\varphi_d/\mathrm{d}s_o + \mathrm{d}\varphi_o/\mathrm{d}s_o)\right]\mathrm{d}s_o}{(1 + \varsigma\kappa_o)\,\mathrm{d}s_o} = \frac{\varepsilon + \varsigma[\kappa(1 + \varepsilon_d) - \bar{\kappa}(1 - \varepsilon_o)]}{1 + \varsigma\kappa_o}. \tag{A.17}$$

The stress corresponding to the UL-strain is referred to as the updated Kirchhoff stress. The axial force and the bending moment due to the updated Kirchhoff stress can be expressed as

$$N = \int_{A_{Po}} \sigma_\varsigma\,\mathrm{d}A_{Po} = E\int_{A_{Po}}\left[\frac{\varepsilon + \varsigma[\kappa(1 + \varepsilon_d) - \bar{\kappa}(1 - \varepsilon_o)]}{1 + \varsigma\kappa_o}\right]\mathrm{d}A_{Po}, \tag{A.18a}$$

$$M = \int_{A_{Po}} \sigma_\varsigma\varsigma\,\mathrm{d}A_{Po} = E\int_{A_{Po}}\left[\frac{\varepsilon\varsigma + \varsigma^2[\kappa(1 + \varepsilon_d) - \bar{\kappa}(1 - \varepsilon_o)]}{1 + \varsigma\kappa_o}\right]\mathrm{d}A_{Po}, \tag{A.18b}$$

in which $A_{Po}$ is the deformed cross-sectional area of the pipe at the equilibrium state.

If the following geometrical properties of the cross-section

$$A^*_{Po} = \int_{A_{Po}} \frac{\mathrm{d}A_{Po}}{1 + \varsigma\kappa_o}, \quad Q^*_{Po} = \int_{A_{Po}} \frac{\varsigma\,\mathrm{d}A_{Po}}{1 + \varsigma\kappa_o}, \quad I^*_{Po} = \int_{A_{Po}} \frac{\varsigma^2\,\mathrm{d}A_{Po}}{1 + \varsigma\kappa_o}. \tag{A.19a–c}$$

are defined, Eqs. (A.18) may be rewritten in the form

$$N = EA^*_{Po}\varepsilon + EQ^*_{Po}[\kappa(1 + \varepsilon_d) - \bar{\kappa}(1 - \varepsilon_o)], \tag{A.20a}$$

$$M = EQ^*_{Po}\varepsilon + EI^*_{Po}[\kappa(1 + \varepsilon_d) - \bar{\kappa}(1 - \varepsilon_o)]. \tag{A.20b}$$

The UL-strain energy due to the UL-strain $\varepsilon_\varsigma$ is measured based on the deformed volume at the equilibrium state of the pipe $\forall_{Po}$. Thus, it can be expressed as

$$U = \int_{\forall_{Po}} \frac{\sigma_\varsigma\varepsilon_\varsigma}{2}\,\mathrm{d}\forall_{Po} = \int_{\forall_{Po}} \frac{\varepsilon_\varsigma^2}{2}\,\mathrm{d}\forall_{Po}. \tag{A.21}$$

Taking the first variation of Eq. (A.21), one obtains

$$\delta U = \int_{\forall_{Po}} E\varepsilon_\varsigma\delta\varepsilon_\varsigma\,\mathrm{d}\forall_{Po} = \int_{s_o}\int_{A_{Po}} \sigma_\varsigma\left[\frac{\delta\varepsilon + \varsigma\delta[\kappa(1 + \varepsilon_d) - \bar{\kappa}(1 - \varepsilon_o)]}{1 + \varsigma\kappa_o}\right]\mathrm{d}A_{Po}\,\mathrm{d}s_o. \tag{A.22}$$

For elastica problems, $\varsigma\kappa_o = \varsigma/r_o \ll 1$, so $1/(1 + \varsigma\kappa_o) \approx 1$. Consequently, Eqs. (A.19) produce $A^*_{Po} \approx A_{Po}$, $Q^*_{Po} \approx 0$, and $I^*_{Po} \approx I_{Po}$. Using these conditions in Eqs. (A.17), (A.20), and (A.22), the constitutive equations of the extensible elastica theory can be obtained as

UL-axial strain:

$$\varepsilon_\varsigma = \varepsilon + \varsigma[\kappa(1+\varepsilon_d) - \bar{\kappa}(1-\varepsilon_o)], \tag{A.23}$$

UL-axial force:

$$N = EA_{Po}\varepsilon, \tag{A.24}$$

UL-bending moment:

$$M = EI_{Po}[\kappa(1+\varepsilon_d) - \bar{\kappa}(1-\varepsilon_o)], \tag{A.25}$$

UL-strain energy:

$$\begin{aligned}\delta U &= \int_{\bar{s}} \{N\delta\varepsilon + M\delta[\kappa(1+\varepsilon_d) - \bar{\kappa}(1-\varepsilon_o)]\}\,\mathrm{d}s_o \\ &= \int_\alpha [N\delta s' + M\delta(\theta' - \bar{\theta}')]\,\mathrm{d}\alpha.\end{aligned} \tag{A.26}$$

Note that

$$\delta\varepsilon = \delta\left(\frac{\mathrm{d}s - \mathrm{d}\bar{s}}{\mathrm{d}s_o}\right) = \delta s'/s'_o, \quad \delta[\kappa(1+\varepsilon_d) - \bar{\kappa}(1-\varepsilon_o)] = \delta\left(\frac{\mathrm{d}\theta}{\mathrm{d}s_o} - \frac{\mathrm{d}\bar{\theta}}{\mathrm{d}s_o}\right) = \delta(\theta' - \bar{\theta}')/s'_o.$$

### *A.3. Eulerian Formulation*

The Eulerian formulation considers total changes from state 1 to 3 by neglecting the intermediate state 2. All changes are measured relative to the final state 3. The development starts by expressing the undeformed and deformed arc lengths of the fibre at any radius $\varsigma$ as

$$\mathrm{d}\bar{s}_\varsigma = (\bar{r} + \varsigma)\,\mathrm{d}\bar{\theta} = \bar{r}\,\mathrm{d}\bar{\theta} + \varsigma(\mathrm{d}\theta - \mathrm{d}\varphi), \tag{A.27a}$$

$$\mathrm{d}s_\varsigma = (r + \varsigma)\,\mathrm{d}\theta. \tag{A.27b}$$

Since $\mathrm{d}\bar{\theta} = (1-\varepsilon)\,\mathrm{d}s/\bar{r}$ and $\mathrm{d}\theta = \mathrm{d}s/r$, Eq. (A.27) may be written in the form

$$\mathrm{d}\bar{s}_\varsigma = (1-\varepsilon)\,\mathrm{d}s + \varsigma\left(\frac{\mathrm{d}s}{r} - \mathrm{d}\varphi\right) = \left(1 - \varepsilon + \varsigma\kappa - \frac{\mathrm{d}\varphi}{\mathrm{d}s}\right)\mathrm{d}s, \tag{A.28a}$$

$$\mathrm{d}s_\varsigma = (1 + \varsigma\kappa)\,\mathrm{d}s, \tag{A.28b}$$

where $\bar{\kappa} = 1/\bar{r}$ and $\kappa = 1/r$ are the curvatures at the undeformed and the displaced states, and

$$\frac{\mathrm{d}\varphi}{\mathrm{d}s} = \frac{\mathrm{d}\theta}{\mathrm{d}s} - \frac{\mathrm{d}\bar{\theta}}{\mathrm{d}\bar{s}}\frac{\mathrm{d}\bar{s}}{\mathrm{d}s} = \kappa - \bar{\kappa}(1-\varepsilon). \tag{A.29}$$

From Definition 4, the EL-strain of the fibre at any radius $\varsigma$ is defined by

$$\varepsilon_\varsigma = \frac{\mathrm{d}s_\varsigma - \mathrm{d}\bar{s}_\varsigma}{\mathrm{d}s_\varsigma} = \frac{(\varepsilon + \varsigma(\mathrm{d}\varphi/\mathrm{d}s))\,\mathrm{d}s}{(1+\varsigma\kappa)\,\mathrm{d}s} = \frac{\varepsilon + \varsigma[\kappa - \bar{\kappa}(1-\varepsilon)]}{1+\varsigma\kappa}. \tag{A.30}$$

The stress corresponding to the EL-strain is referred to as the Cauchy stress. The axial force and bending moment due to the Cauchy stress can be expressed as

$$N = \int_{A_P} \sigma_\varsigma\,\mathrm{d}A_P = E\int_{A_P}\left[\frac{\varepsilon + \varsigma[\kappa - \bar{\kappa}(1-\varepsilon)]}{1+\varsigma\kappa}\right]\mathrm{d}A_P, \tag{A.31a}$$

$$M = \int_{A_P} \sigma_\varsigma\varsigma\,\mathrm{d}A_P = E\int_{A_P}\left[\frac{\varepsilon\varsigma + \varsigma^2[\kappa - \bar{\kappa}(1-\varepsilon)]}{1+\varsigma\kappa}\right]\mathrm{d}A_P, \tag{A.31b}$$

in which $A_P$ is the deformed cross-sectional area of the pipe at the displaced state.

If the following geometrical properties of the cross-section

$$A_P^* = \int_{A_P} \frac{\mathrm{d}A_P}{1+\varsigma\kappa}, \tag{A.32a}$$

$$Q_P^* = \int_{A_P} \frac{\varsigma\,\mathrm{d}A_P}{1+\varsigma\kappa}, \tag{A.32b}$$

$$I_P^* = \int_{A_P} \frac{\varsigma^2\, \mathrm{d}A_P}{1+\varsigma\kappa}. \tag{A.32c}$$

are defined, Eqs. (A.31) may be rewritten in the form

$$N = EA_P^*\varepsilon + EQ_P^*[\kappa - \bar{\kappa}(1-\varepsilon)], \tag{A.33a}$$

$$M = EQ_P^*\varepsilon + EI_P^*[\kappa - \bar{\kappa}(1-\varepsilon)]. \tag{A.33b}$$

The EL-strain energy due to the EL-strain $\varepsilon_\varsigma$ is measured with respect to the deformed volume at the displaced state of the pipe $\forall_P$. Thus, its expression is given by

$$U = \int_{\forall_P} \frac{\sigma_\varsigma \varepsilon_\varsigma}{2}\, \mathrm{d}\forall_P = \int_{\forall_P} \frac{\varepsilon_\varsigma^2}{2}\, \mathrm{d}\forall_P. \tag{A.34}$$

Taking the first variation of Eq. (A.34), one obtains

$$\delta U = \int_{\forall_P} E\varepsilon_\varsigma \delta\varepsilon_\varsigma\, \mathrm{d}\forall_P = \int_s \int_{A_P} \sigma_\varsigma \left[\frac{\delta\varepsilon + \varsigma\delta[\kappa - \bar{\kappa}(1-\varepsilon)]}{1+\varsigma\kappa}\right] \mathrm{d}A_P\, \mathrm{d}s. \tag{A.35}$$

For elastica problems, $\varsigma\kappa = \varsigma/r \ll 1$, thus $1/(1+\varsigma\kappa) \approx 1$. As a result, Eqs. (A.32) yield $A_P^* \approx A_P, Q_P^* \approx 0$, and $I_P^* \approx I_P$. Substituting these conditions in Eqs. (A.30), (A.33), and (A.35), the constitutive equations of the extensible elastica theory are obtained as

EL-axial strain:

$$\varepsilon_\varsigma = \varepsilon + \varsigma[\kappa - \bar{\kappa}(1-\varepsilon)], \tag{A.36}$$

EL-axial force:

$$N = EA_P\varepsilon, \tag{A.37}$$

EL-bending moment:

$$M = EI_P[\kappa - \bar{\kappa}(1-\varepsilon)], \tag{A.38}$$

EL-strain energy:

$$\delta U = \int_s \{N\delta\varepsilon + M\delta[\kappa - \bar{\kappa}(1-\varepsilon)]\}\, \mathrm{d}s = \int_\alpha [N\delta s' + M\delta(\theta' - \bar{\theta}')]\, \mathrm{d}\alpha. \tag{A.39}$$

Note that

$$\delta\varepsilon = \delta\left(\frac{\mathrm{d}s - \mathrm{d}\bar{s}}{\mathrm{d}s}\right) \approx \delta s'/s', \quad \delta[\kappa - \bar{\kappa}(1-\varepsilon)] = \delta\left(\frac{\mathrm{d}\theta}{\mathrm{d}s} - \frac{\mathrm{d}\bar{\theta}}{\mathrm{d}s}\right) \approx \delta(\theta' - \bar{\theta}')/s'.$$

## References


Atanackovic, T.M., 1997. Stability Theory of Elastic Rods. World Scientific, Singapore.

Bernitsas, M.M., Kokarakis, J.E., 1988. Importance of nonlinearities in static riser analysis. Applied Ocean Research 10, 2–9.

Bernitsas, M.M., Kokarakis, J.E., Imron, A., 1985. Large deformation three-dimensional static analysis of deep water marine risers. Applied Ocean Research 7, 178–187.

Burgess, J.J., Triantafyllou, M.S., 1988. The elastic frequencies of cables. Journal of Sound and Vibration 120, 153–165.

Chakrabarti, S.K., 1990. Nonlinear Methods in Offshore Engineering. Elsevier, Amsterdam.

Chakrabarti, S.K., Frampton, R.E., 1982. Review of riser analysis techniques. Applied Ocean Research 4, 73–90.

Chucheepsakul, S., Huang, T., 1994. Influence of transported mass on the equilibrium configuration of risers. Proceedings of the Fourth International Offshore and Polar Engineering Conference (ISOPE), Vol. 2, pp. 246–249.

Chucheepsakul, S., Huang, T., 1997. Effect of axial deformation on natural frequencies of marine cables. Proceedings of the Seventh International Offshore and Polar Engineering Conference (ISOPE), Vol. 2, pp. 131–136.

Chucheepsakul, S., Monprapussorn, T., 2001. Nonlinear buckling of marine elastica pipes transporting fluid. International Journal of Structural Stability and Dynamics 1, 333–365.

Chucheepsakul, S., Huang, T., Laohaporjanat, P., 1995. Effects of axial deformation on the equilibrium configurations of marine cables. Proceedings of the Fifth International Offshore and Polar Engineering Conference (ISOPE), Vol. 2, pp. 244–248.

Chucheepsakul, S., Huang, T., Monprapussorn, T., 1999. Influence of transported fluid on behaviour of an extensible flexible riser/pipe. Proceedings of the Ninth International Offshore and Polar Engineering Conference (ISOPE), Vol. 2, pp. 286–293.

Chung, J.S., Cheng, B.-R., 1996. Effects of elastic joints on 3-D nonlinear responses of a deep-ocean pipe: modeling and boundary conditions. International Journal of Offshore and Polar Engineering 6, 203–211.
Chung, J.S., Whitney, A.K., 1983. Dynamic vertical stretching oscillation of a deep-ocean mining pipe. ASME Journal of Energy Resources Technology 105, 195–200.
Chung, J.S., Cheng, B.-R., Huttelmaier, H.-P., 1994. Three-dimensional coupled responses of a vertical deep-ocean pipe: Part I. Excitation at pipe ends and external torsion. International Journal of Offshore and Polar Engineering 4, 320–330.
Doll, R.W., Mote, C.D., 1976. On the dynamic analysis of curved and twisted cylinders transporting fluids. ASME Journal of Pressure Vessel Technology 98, 143–150.
Ertas, A., Kozik, T.J., 1987. A review of current approaches to riser modeling. ASME Journal of Energy Resources Technology 109, 155–160.
Fung, Y.C., 1994. A First Course in Continuum Mechanics. Prentice-Hall, Englewood Cliffs, NJ.
Garrett, D.L., 1982. Dynamic analysis of slender rods. ASME Journal of Energy Resources Technology 104, 302–306.
Goodman, T.R., Breslin, J.P., 1976. Static and dynamics of anchoring cable in waves. Journal of Hydronautics 10, 113–120.
Gregory, R.W., Païdoussis, M.P., 1966. Unstable oscillation of tubular cantilevers conveying fluid. I. Theory. Proceedings of the Royal Society (London) A 293, 512–537.
Holmes, P.J., 1978. Pipes supported at both ends cannot flutter. ASME Journal of Applied Mechanics 45, 619–622.
Housner, G.W., 1952. Bending vibrations of a pipe line containing flowing fluid. ASME Journal of Applied Mechanics 19, 205–208.
Huang, T., 1992. A static equilibrium formulation including axial deformation for marine cables. Proceedings of the Second International Offshore and Polar Engineering Conference (ISOPE), Vol. 2, pp. 252–255.
Huang, T., 1993. Kinematics of transported mass inside risers and pipes. Proceedings of the Third International Offshore and Polar Engineering Conference (ISOPE), Vol. 2, pp. 331–336.
Huddleston, J.V., 1981. Computer analysis of extensible cables. ASCE Journal of Engineering Mechanics Division 107, 27–37.
Irani, M.B., Modi, V.J., Weit, F., 1987. Risers dynamics with internal flows and nutation damping. Proceedings of Sixth International Offshore Mechanics and Arctic Engineering Symposium, Vol. 3. ASME, Houston, pp. 119–125.
Jain, A.K., 1994. Review of flexible risers and articulated storage systems. Ocean Engineering 21, 733–750.
Lin, H.P., Perkins, N.C., 1995. Free vibration of complex cable/mass system: theory and experiment. Journal of Sound and Vibration 179, 131–149.
Moe, G., Chucheepsakul, S., 1988 The effect of internal flow on marine risers. Proceedings of the Seventh International Offshore Mechanics and Arctic Engineering Symposium, Vol. 1. ASME, Houston, pp. 375–382.
Munson, B.R., Young, D.F., Okiishi, T.H., 1994. Fundamentals of Fluid Mechanics. Wiley, Toronto.
Païdoussis, M.P., 1970. Dynamics of tubular cantilevers conveying fluid. Journal of Mechanical Engineering Science 12, 85–103.
Païdoussis, M.P., 1998. Fluid-Structure Interactions: Slender Structures and Axial Flow, Vol. 1. Academic Press, New York.
Patel, H.M., Seyed, F.B., 1989. Internal flow-induced behaviour of flexible risers. Engineering Structures 11, 266–280.
Patel, H.M., Seyed, F.B., 1995. Review of flexible riser modeling and analysis techniques. Engineering Structures 17, 293–304.
Shames, I.H., 1992. Mechanics of Fluids. McGraw-Hill, Singapore.
Shih, B., Tadjbakhsh, I.G., 1984. Small-amplitude vibrations of extensible cables. ASCE Journal of Engineering Mechanics 110, 569–576.
Sparks, C.P., 1984. The influence of tension, pressure and weight on pipe and riser deformations and stresses. ASME Journal of Energy Resources Technology 106, 46–54.
Thompson, J.M.T., Lunn, T.S., 1981. Static elastica formulations of a pipe conveying fluid. Journal of Sound and Vibration 77, 127–132.
Timoshenko, S.P., Goodier, J.N., 1984. Theory of Elasticity. McGraw-Hill, Singapore.
Tjavaras, A.A., Triantafyllou, M.S., 1996. Shock waves in curved synthetic cables. ASCE Journal of Engineering Mechanics 122, 308–315.
Tjavaras, A.A., Zhu, Q., Liu, Y., Triantafyllou, M.S., 1998. The mechanics of highly extensible cables. Journal of Sound and Vibration 213, 709–737.
Triantafyllou, M.S., Yue, D.K.P., 1994. Damping amplification in highly extensible hysteretic cables. Journal of Sound and Vibration 186, 355–368.
Wu, M.C., Lou, J.Y.K., 1991. Effects of rigidity and internal flow on marine riser dynamics. Applied Ocean Research 13, 235–244.